Accepted Manuscript

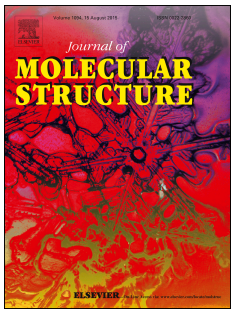

Synthesis and characterization for novel Cu(II)-thiazole complexes-dyes and their usage in dyeing cotton to be special bandage for cancerous wounds

Nashwa El-Metwaly, Ismail Althagafi, Abdalla M. Khedr, Jabir H. Al-Fahemi, Hanadi A. Katouah, Aisha S. Hossan, Aisha Y. Al-Dawood, Gamil A. Al-Hazmi

PII: S0022-2860(19)30650-7

DOI: https://doi.org/10.1016/j.molstruc.2019.05.080

Reference: MOLSTR 26587

To appear in: *Journal of Molecular Structure*

Received Date: 14 April 2019

Revised Date: 15 May 2019

Accepted Date: 19 May 2019

Please cite this article as: N. El-Metwaly, I. Althagafi, A.M. Khedr, J.H. Al-Fahemi, H.A. Katouah, A.S. Hossan, A.Y. Al-Dawood, G.A. Al-Hazmi, Synthesis and characterization for novel Cu(II)-thiazole complexes-dyes and their usage in dyeing cotton to be special bandage for cancerous wounds, *Journal of Molecular Structure* (2019), doi: https://doi.org/10.1016/j.molstruc.2019.05.080.

Synthesis and characterization for novel Cu(II)-thiazole complexes-dyes and their usage in dyeing cotton to be special bandage for cancerous wounds

Nashwa El-Metwaly[1,2*], Ismail Althagafi[1], Abdalla M. Khedr[1,3], Jabir H. Al-Fahemi[1], Hanadi A. Katouah[1], Aisha S. Hossan[4], Aisha Y. Al-Dawood[1], Gamil A. Al-Hazmi [4,5]

[1]*Chemistry Department, College of Applied Sciences, Umm Al-Qura University, Makkah, Saudi Arabia*
[2]*Chemistry Department Faculty of Science, Mansoura University, Mansoura, Egypt*
[3]*Chemistry Department, Faculty of Science, Tanta University, Tanta, Egypt*
[4]*Chemistry Department, Faculty of Science, King Khalid University, P.O. Box 9004, Abha, Saudi Arabia*
[5]*Chemistry Department, Faculty of Applied Sciences, Taiz University, P.O. Box 82, Taiz, Yemen*

Abstract

New series of Cu(II)-thiazole complexes were synthesized using variable p-substituted, *N*-aryl-2-oxo-2-(thiazol-2-ylamino)-acetohydrazonoyl cyanide. All new syntheses were elucidated by, analytical, spectral and conformational study. The binuclear feature (2M:1L), was proposed for all complexes, through mono-negative tetra-dentate chelation mode in octahedral or square-planer geometry. The formulae of chosen compounds, were confirmed by, ^{1}HNMR and mass spectral analysis. The ideal distribution for atomic-skeletons, was performed utilizing Gaussian09 software, to confirm the bonding mode. Also, substantial parameters were extracted from output-files (log &chk), beside others calculated based on frontier energy gaps. The superiority of Cu(II) complexes, was predicated from such conformational study. Also and by applying MOE module, the docking process was performed for most syntheses against selected pathogen proteins (1miu, 4k9g and 5jm5), which have been tested practically in application. The extracted docking-data, showed clear superiority and promising efficiency for Cu(II) complexes as anticancer drugs compared to free derivatives. Traditional screening was conducted over new complexes against three carcinoma cell lines (HCT-116, MCF-7 & HepG-2) as well as healthy cell line (HSF). IC_{50} values showed considerable toxicity of Cu(II)-4e complex versus HCT-116 cell line. The antitumor screening was conducted over cotton fabric after dyeing by complexes, to test the degree of success to be used as a special bandage for cancerous wounds. The most lighted observation was, the effect of released-pigmenting complex on colon cancer cell line, while the absence of any effect on healthy cell. Also, the released-pigment, controlled the pH of cancerous wound, which is significantly preferable.

Keywords: Cu(II)-thiazole complexes, bandage for cancerous wounds, CT-DNA, molecular Docking, DFT/B3LYP

[*]*Corresponding author:* Prof. Nashwa M. El-Metwaly, *E- mail address: n_elmetwaly00@yahoo.com, Telephone No.: +966538553123*

1. Introduction

For many years, the heterocyclic compounds containing O, N, and S, displayed magnificent importance in medicinal and chemical applications[1,2]. They are widely applied as cosmetics, perfumes, food additives, pharmaceuticals, optical brighteners, laser and fluorescent and dyes[3]. Thiazole derivatives have enhanced antimicrobial activities towards various pathogens including *Helicobacter pylori* and *Mycobacterium tuberculosis*[4]. These thaisole compounds, have also good anti-cholinesterase, anti-cancer, anti-analgesic, anti-inflammatory activities[5]. Transition metals have incorporated with numerous biological processes that are animated to life processes[6]. Hence, they can coordinate with N- or O-terminals from proteins in a assortment of models, and so, play a peppy role biological system such as the utility and conformation of living macromolecules [7]. Schiff bases involving imino moieties (>C=N–) and their complexes have been exceedingly reported to display a distinction of motivating biological effectiveness such as anti-inflammatory, antimicrobial, antifungal, antitumor, analgesic effects, anti-proliferative, and anticancer activities[8]. Transition metal ion complexes, containing different bioactive ligands, are often more efficacious regarding pharmaceutical and biological applications compared with the free ligands [9]. Additionally, Schiff bases containing thiazole nucleus are expected to exhibit great biological activities especially as antitumors [10]. Metal complexes as therapeutic antitumor agents have been widely applied following the success of cis-platin. Recently, cis-platin has been identified as one of the most extensively applied antitumor drugs over the world, elevated efficiency for ovarian and testicular cancers, in the treatment of bronchogenic, oropharyngeal, bladder, cervical, and carcinoma species [11]. Different complexes based on platinum ions are clinically applied in order to help the inducement of cancer cells death. Platinum compounds have toxic effects, despite the positive effects of them in killing cancer cells [12]. We have synthesized different other metal complexes and tested for their anticancer and other bio-activities [13,14], to overcome the disadvantages of platinum complexes. Furthermore, Cu(II) complexes derived from Schiff bases have been reported as a promising potential chemotherapeutic agents [15]. From all previously reported, especially that interested in Cu(II) complexes, they were fully succeeded in biological applications concerning various pathways. From such point, and now we interested in synthesis of new thiazole dyes, which utilized to synthesize their corresponding Cu(II) complexes. After completing synthesis, all verification tools (analytical, spectral and conformational theoretical) were implemented to extract full characterization bases. Furthermore and concerning the application part, we conduct test to enhance anti-cancer impact by create innovative design for special bandage that gains three prominent features. Such features as, close the wounds, eliminate bacteria from cancer mass, which allowing chemotherapy to reach their target. Moreover, keep cancer cells under stable

concentration of compound-released from bandage under the acidic conditions which already created by cancer cells themselves.

2. Experimental part

2.1. Chemicals used

The reagents used to prepare diazonium salts as, $NaNO_2$, HCL, aniline, 4-toluidine, 4-anisidine, 4-acetoaniline and 4-chloroaniline, which were purchased from Sigma & Aldrich. Thiazolyl-cyanoacetamide, which used for diazo-coupling, was PDH. $CuCl_2$. $2H_2O$ is a Fluka product which used in complexation. While, the chemical of antitumor study were, SulphoRhodamine-B (SRB), were purchased from Sigma Chemical Co. (St. Louis, MO, USA). Culture media and growth supplements were purchased from Gibco / Life Technologies Co, (Carlsbad, CA, USA). Cell culture vessels were purchased from Nunc Co. (Roskilde, Denmark). All solvents as, ethanol, methanol, DMF, DMSO were PDH and used without previous treatments.

2.2. Synthesis

2.2.1. Synthesis of *N*-aryl-2-oxo-2-(thiazol-2-ylamino)-acetohydrazonoyl cyanide derivatives 4a-e

The preliminary step was the synthesis of diazonium salt, in which an aqueous solution of 0.21g sodium nitrite (in 10mL H_2O) was added gradually to cold solution (0□) of the aromatic amine (0.003 mol) (namely; aniline, 4-toluidine, 4-anisidine, 4-acetoaniline and 4-chloroaniline in 3 mL conc. HCl. Secondly, a diazocoupling process was executed after the addition of each diazonium salt solution to to a cold solution (0□) of thiazolyl-cyanoacetamide derivative **3** (0.003 mol, 0.50 g) in pyridine (30 mL), with constant stirring till 2h (**Scheme 1**). The solid that obtained upon dilution with 10 mL cold water was filtered off. Recrystallization process was carried out from EtOH-DMF (1:1) mixture, to pick up acetohydrazonoyl cyanide dyes **4a-e[**16]. The colored derivatives **4a-e** were yielded by 67-76% and their melting points are ranges of, 248-250, 228-230, 208-210, 268-270 and 252-254□, respectively. The elements content and IR spectral study proposed the formulae of dyes **4a-e (Fig. 1S)**, which suggested to found in tautomeric forms (keto/enol). ^{1}H & ^{13}C NMR spectral analysis (**Fig. 1**&**2S**) were accomplished for two selected derivatives (4b &4c, in d_6-DMSO), which asserted on formulae suggested. The ^{1}H NMR spectrum of 4b, H-TTAC derivative displayed signals at; δ = 2.31 (s, 3H, CH_3), 7.20 (d, *J* = 8.4 Hz, 2H, Ar-H), 7.28 (d, *J* = 3.6 Hz, 1H, thiazole-H5), 7.55 (d, *J* = 3.6 Hz, 1H, thiazole-H4), 7.74 (d, *J* = 8.4 Hz, 2H, Ar-H), 12.05 (s, 1H, NH or OH), 12.39 (s, 1H, NH).). Its ^{13}C NMR spectrum displayed signals at; δ = 21.60, 108.44, 112.73, 117.13 (2C), 124.73, 130.72 (2C), 131.76, 140.67, 154.46, 160.44, 163.46 ppm. While, the ^{1}H NMR spectrum of 4c, H-ATAC displayed signals at; δ =3.78 (s, 3H, OCH_3), 7.00 (d, *J* = 8.4 Hz, 2H, Ar-H), 7.28 (d, *J* = 3.6 Hz, 1H, thiazole-

H5), 7.55 (d, *J* = 3.6 Hz, 1H, thiazole-H4), 7.80 (d, *J* = 8.4 Hz, 2H, Ar-H), 12.31 (s, 1H, NH or OH). Its ^{13}C NMR spectrum displayed signals at δ = 55.92, 107.28, 111.72, 115.29 (2C), 118.88 (2C), 126.72, 129.81, 136.17, 152.91, 160.90, 164.54 ppm.

Scheme. 1.

2.2.2. Synthesis of Cu(II)-thiazole complexes

The complexes were synthesized by using equi-molar addition of $CuCl_2$. $2H_2O$ (2mmol, 0.341g) to each corresponding thiazole derivative **4a-e** in ethanolic solution. The reaction mixtures were heated under reflux from 3-5h, the solid complexes were precipitated. All hot solutions were filtered off, washed by ethanol and followed by diethyl ether. The complexes were dried in vacuum desiccators under $CaCl_2$. All complexes are stable, insoluble in common organic solvents but completely soluble in DMSO and DMF, also having high m.p. over 300 ^{o}C.

2.2.3. Cotton-bandage pigmentation

0.2g from each prepared complex was dissolved in few drops of DMF and completed to 20 mL by ethanol, then the dye bath was adjusted to pH=6 and heated till 90^{o}C, after that, 1g from cotton fabric was immersed. The dyeing solution was stirred over 60 min, after that cool the dye bath. Followed by washing pigmented cotton by distilled water and in aqueous solution containing 1 g/L detergent for 10 min at 90^{0}C by a ratio of 20:1, then the dyed cotton-pieces are ready for application [17].

2.3. DNA binding

The degree of binding efficiency for new triazole derivatives towered CT-DNA has been investigated using spectrophotometric method. 50 mg of CT-DNA were dissolved overnight in bi-distilled water (pH= 7.0) through stirring and hold at 4 ^{o}C. A buffering solution (Tris - HCl buffer) was prepared by mixing solutions of 5.0 mM tris(hydroxymethyl)-aminomethane and 50 mM NaCl (in bi-distilled water, pH= 7.0). A definite concentration from CT-DNA was prepared in Tris-HCl buffer. Such, gave absorption at 260 and 280 nm by ratio; A260/A280 equal to 1.8-1.9 range, which is attributing to DNA free from protein [18]. A known molar absorpitivity coefficient (6600 $M^{-1}cm^{-1}$) for DNA at 260 nm, was used to estimate its concentration spectrophotometricaly (5.25×10^{-4} M). 200- 900 nm was the scanning range for measurements using 1cm quartz cuvette at 25°C. A fixed concentration from each compound (6a-6e) was used (2.5×10^{-5}M). Then a gradual addition for CT-DNA amount till the concentration raise from 0.00 to 1.58 × 0^{-4}mol L^{-1} was done. The amounts used from CT-DNA, were added also to each referenced cells include buffer solution to eliminate the absorption of free DNA.

The intrinsic binding constant (K_b) of each compound towards DNA was extracted by using; [DNA] / (ϵa − ϵf) = [DNA] / (ϵb − ϵf) + 1/K_b (ϵa − ϵf) equation [19]. Where; [DNA] is the molar concentration of DNA, ϵa is the extinction coefficient observed for Aobs / [compound] at used DNA concentration. Moreover, ϵf is the extinction coefficient for each free compound (**4a-e**), ϵb is the extinction coefficient of the compound at full bonding towards DNA. K_b can be determined from the plots [DNA] / (ϵa − ϵf) vs. [DNA] through the ration; slope / intercept.

2.4. Analytical techniques

Elemental analysis of carbon, hydrogen, nitrogen, and sulfur of all compounds in concern, were determined using Perkin-Elmer 2400 CHN Elemental Analyzer. Known referenced method [20], was utilized to estimate the copper and chloride contents in synthesized complexes. The molar conductance of tested complexes was performed by JENWAY model 4070 Conductance Bridge. ^{1}HNMR and IR (using KBr disc) spectra were conducted over Burker 400MHz and JASCO FT-IR-4100 spectrophotometers (400–4000 cm^{-1}), respectively. Electronic absorption (UV/Vis) spectra (in DMSO) and magnetic susceptibility were estimated at room temperature by applying UV_2 Unicam UV/Vis spectrophotometer and Johnson Matthey Magnetic Susceptibility Balance. Mass spectral analysis was obtained at 70 ev by, AEIMS 30 mass spectrometer by heating rate 40°C/min, covering range of mass 50-1000. XRD patterns were obtained by using X-ray diffractometer (GNR, APD2000PRO, Italy) with graphite mono-chromator over a range of $10^\circ < 2\theta < 90^\circ$ at scanning rate by 0.03° min^{-1} under Cu/Kα1 radiation source. SEM images were extracted by implementing Joel JSM-6390 technique. TGA study for complexes was executed by Shimadzu Thermal Analyzer by applying constant heating rate (10 ^oC min^{-1}) up to 20-900^oC range, under N_2. Conformational analysis and MOE docking were conducted by Gaussian09 program and MOE module (version 2015), respectively. The biological activity test was screened in specialized laboratory.

2.5. Conformational techniques

2.5.1. DFT/B3LYP method

All structural forms were adjusted by Gaussian 09 program [21], to build the best orientation for functional groups, which confirms the bonding mode. The most fitted method was DFT using 3-21G base set in ethanol, as a default solvent, in simulation with synthesis, which already done in it. The basic files were acquired (log & chk) and visualized over Gauss-View program screen [22]. Basic parameters were estimated based on E_{HOMO} & E_{LOMO}, and others were taken from files [23, 24].

2.5.2. Molecular docking study

The crystal structures of 1miu, 4k9g and 5jm5 proteins in PDB format, were docked with most synthesizes, for simulation. 1miu is a breast cancer susceptibility gene2 (1miu), 4k9g is a novel inhibitor of macrophage migration, which shows efficacy in melanoma and colon cancer models, while 5jm5 is an AKR1C3 based Pro-drug TH3424, which has potent anti-tumor activity against liver cancer. The introductory step, is the addition of hydrogen–atoms, after removing water molecules around the helix. The charges and parameters were estimated by MMFF94x force field, after fixing the potential. Implementing MOE module and after generating alpha-site sphere on site finder, the tested compounds as MDB files, were docked on surface interior-grooves [25]. The scoring energy in MOE module, was estimated using London dG scoring function and also upgraded by two unrelated-refinement by triangle Matcher methods. The tested compounds were optimized, to minimize the energy content, which led to best binding ability, after that the compounds oriented for analysis. Database browser was used to compare the docking efficiency for tested co-crystals. From binding free energy score and hydrogen bonds of co-crystals toward amino acids in protein-receptors, the rank of binding affinity, was estimated. The hydrogen bonds were evaluated by measuring its length, which did not exceed than 3.5 Å. The type of bonded centers and the nature of bonding between crystal structures and protein-receptors, were estimated, through mapping the receptor surface.

2.6. Usage of dyed-bandage in cancerous-wounds

2.6.1. Cell culture and viability

Human hepatic carcinoma (HepG-2), breast (MCF-7) colon (HCT116) and normal fibroblast cells (HSF) were obtained from Viscera (Giza, Egypt). The cytotoxicity and anticancer activities of prepared Cu(II) complexes (4a-e) were tested against three carcinoma cell lines in addition to one normal cell line (HSF) using SulphoRhodamine-B (SRB) assay. Different cancer and normal cell lines exposed to concentration range of, 0.01 to 100 µg/ml from complexes, then incubated (in 5% CO_2 humidified incubator) at 37 °C for 72 h. Treated cells were fixed with TCA (10%) for 1h at 4°C. Subsequently, to remove TCA, cells were washed with water many times, and then 0.4% SRB solution was used to stain cells in dark place for 10 min. Stained cells washed with 1% glacial acetic acid. Finally, to dissolve SRB-stained cells, Tris–HCl was used. After drying overnight, the color intensity of remained cells was measured at 540nm by Elisa[26], in comparing to positive control (doxorubicin).

2.6.2. The impact of released complexes on cells

In attempt to evaluate the impact of different Cu(II) complexes (4a-e) loaded on cotton, on colon(HCT-116), liver(HepG-2) and breast (MCF-7) cancer cell lines as well as normal cell lines(HFS). All cells were incubated with the same number of fibers (five fibers for each) isolated from the loaded cottons for 72h in 5% CO2 humidified incubator. The cellular morphological-modifications were controlled under inverted microscope every 24h, to get a correlation between, release amount of complex from the cotton bandage, against the change of medium-pH. The data were analyzed using Sigma Plot version 14.0.

3. Results and discussion

3.1. Analytical data

General characteristics of thiazole ligands and their Cu(II) complexes (4a-e) were displayed in Table 1. The data presented confirm the formation of 2:1 (Cu:L) molar stoichiometry for all synthesized complexes. The molecular formulae of all synthesizes were built based on elemental analysis and mass spectral analysis for elected synthesizes, which matches directly to mathematical prediction. The complexes have non-hygroscopic nature, high m. p. up to 300 ^{o}C and insoluble in traditional organic solvents but excellently soluble in DMSO solvent. Two estimated values were 5.12 and 6.82 Ω^{-1} cm^{2} mol^{-1}, for complexes Cu(II)-4a and Cu(II)-4d, respectively. This values support their non-electrolytic nature, which agrees comfortably with covalent nature of chloride that analogues to its ionic one. Whilst, Cu(II)-4e complex, displays molar-conductance value of 55.19 Ω^{-1} cm^{2} mol^{-1}, which matches conducting feature of one mobile anion [27].

3.2. Thiazole (4a-e) synthesis Mechanism

Thiazolyl-cyanoacetamides (thiazole-NHCOCH$_2$CN) are known by their high reactivity with poly-functional features. This due to possessing electrophilic and nucleophilic groups as, NH &CH$_2$, which arranged by, CH$_2$ > NH. From this perspective, we synthesized new cyanoacetamido-thiazole derivatives dyes (4a-e), with variable p-substituents, which changed between electron-donating to electron-withdrawing groups, for discrimination. 2-Cyanoacetamido-thiazole **(1)**, a starting material that was prepared by heating 2-aminothiazole with cyanoacetic acid in the presence of acetic anhydride according to referenced procedure [16]. The reactivity of active methylene-group in 2-cyanoacetamido-thiazole **(1**), was tested towards variable-substituting diazonium salts. Diazocouplig reaction, which carried out between cyanoacetamide (**1**) and diazonium salts derived from different aniline derivatives (in pyridine), was ended by respective thiazolyl-hydrazonyl nitrile dyes, **4a-e (Scheme 1).** The reaction was proceeded

at most reactive site (methylene group) rather than another possible site (thiazole-C5). The analytical and spectral data for compounds **4a-e**, consistent with the proposed structures. IR spectra displayed absorption bands at, 3460-3150, 2206-2220 and 1691-1652 cm^{-1} regions, which compatible with υN-H or υO-H , υC≡N and υC=O groups, respectively. ^{1}H NMR spectrum of **4c** (as example) showed signals confirming the atomic skeleton proposed. A singlet signal (3H) appeared at, δ= 3.78 ppm assigns for methoxy group (-O-CH_3). Doublet signals appeared at, δ= 7.00 and 7.80 ppm identified the aromatic protons. While, the protons of thiazole-C_5 and thiazole-C_4 were resonated at 7.28 (doublet) and 7.55 ppm (doublet), respectively. Moreover, a singlet signal appeared at, δ= 12.31 ppm assigns for NH or OH (in enol tautomer).

3.3. The mode of bonding

In order to recognize the coordination sites in thiazole ligands, which chelate to Cu(II) ions, the IR spectra of complexes. Cu(II)-thiazole complexes (4a-e**)** were contributed in deliberate comparison with that of free ligands. Fundamental spectral bands for all couples (derivative and its complex) were extracted and gathered in Table 2. With respect to thiazole derivatives, the bands appeared at; 3460-3420, 3296-3150, 1655-1590, and 1691-1652 cm^{-1} ranges, assign for υ(OH) (in enol-form), υ(NH)s, second υ(NH)s, nitrile function υ(C≡N), and υ(C=O), respectively. While, comparative study between each free ligand and its coupled complex reveal such common information as;. i) Complete obscure for υ(C=O) vibration, suggests its coordination with Cu(II) ions after de-protonation. ii)Also, vanishing υNH (amide), is a further support for enolization during complexation process. iii) Non-obvious shift of υ(C≡N) bands, denotes complete exclusion for CN group from coordination sphere. iv) ν(C-O) vibration band which appeared at, 1160-1089 cm^{-1} range before complexation, after that, was appeared with great shift in all complexes, due to coordination of enol-tautomer [28]. v) While, the vibration of υ(C-S), which already presented at; 720-671 cm^{-1} rang, was appeared more-or less un-shifted in all complexes. This a clear evidence for its ruling out from coordination, as theoretically expected. From all previously reported, a mono-negative tetra-dentate mode of bonding contributing two central atoms , was the only mode proposed for all complexes. Moreover, the appearance of new bands at; 691-675 and 860-812 cm^{-1} ranges, that assign to $\delta_w(H_2O)$ and $\delta_r(H_2O)$ of occluded solvent molecules, respectively [29]. In addition to new vibrational bands at, 578-566 and 506-492 cm^{-1}, which may attribute to ν(M-O) and ν(M-N), respectively, were the final evidence for coordination feature.

3.4. Electronic spectral inspection

Essential spectral bands for all investigated compounds were extracted from UV-Vis spectra to assert on structural formula of interested complexes. Moreover, other spectral data as, oscillator strength, and molar absorpitivity, were estimated for perfectly soluble compounds for $1x10^{-4}$ ML^{-1}(in DMSO) concentration (Table 3). Most of electronic transitions inside thiazole ligands, were obviously affected by p-substituent's especially bands related to C=N group. $\pi\rightarrow\pi^*$ transitions, which observed at 35,471-37,120 and 28,710-35,184 cm^{-1}, can be attributed to C=O and C=N bands, respectively. Furthermore, $n\rightarrow \pi^*$ transitions were appeared within 22,910-30,178 cm^{-1} range. Such range, is highly contributing with visible region, which considered the logical result for high conjugation inside ligands-structures [30]. In common, blue shifts were observed for all intra-ligand transitions upon complex formation, which seems to be an excellent evidence for coordination process. Also, the values of molar absorpitivities computed for the first transition inside ligands, suffer reduction in the corresponding complexes due to charge transfer transitions (L→M). Two structural geometries were suggested for five inspected Cu(II) complexes; square-planer configurations for Cu(II)-4a, Cu(II)-4d, and Cu(II)-4e complexes. While, an octahedral configuration for Cu(II)-4b, and Cu(II)-4c complexes. These variable features originally depend on various recorded electronic transitions, which strongly conjugating with p-substituent's effect. Spectra of $[Cu_2Cl_3(PTAC)(H_2O)]H_2O$, $[Cu_2Cl_3(AcTAC)(H_2O)]H_2O$, and $[Cu_2Cl_2(CTAC)(H_2O)_2]Cl.H_2O$ complexes exhibited significant d-d transitions consequently at, 18,671;16,512, 18,326;16,521, and 18,056; 16,452 cm^{-1}. These transitions assign to $^2B_1g\rightarrow{}^2A_1g$ and $^2B_1g\rightarrow{}^2Eg$ electronic transitions, respectively [31]. These transitions confirmed the geometry of square-planer arrangement proposed. Whilst, the spectra of $[Cu_2Cl_3(TTAC)(H_2O)_4]2H_2O$, and $[Cu_2Cl_2(CTAC)(H_2O)_2]Cl.H_2O$ complexes, displayed two significant transitions at, 21,218;18,821 and 22,451;19,193 cm^{-1}, respectively. These bands were assigned to $^2B_1g\rightarrow{}^2Eg$ and $^2B_1g\rightarrow{}^2B_2g$ transitions, which supporting distorted octahedral arrangements around cooper atoms [32]. Magnetic moment values of the five complexes (μ_{eff} =1.60-1.63 BM) were found less than the well-known values for one unpaired electron [32]. These subnormal values, may be point to significant metal-metal interaction inside binuclear complex. All optimized structural forms for Cu(II) complexes, were displayed in figure 2.

3.5. Mass spectral analysis

To be satisfied with the chemical formulae proposed, the mass spectral analysis was performed for two representative examples (Fig. 3), up to m/z = 1000. H-PTAC (4a) was the selected derivative for the first mass analysis and its spectrum displayed, a molecular ion peak (M^+) with exact mass at m/z= 271.05(100%)(calcd. 271.30). Also, the apparent split of molecular ion peak, which recorded at, 272.06(13.1%), 273.05(4.8%), 272.05(2.6%) and 273.06(1.1%), may point to M^++1 and M^++2.

Through the influence of electron bombardment, the most fitted fragmentation pathway was exhibited in **Scheme 2**. The other spectrum was executed for Cu(II)-4c complex, to serve as a common evidence for all formulae proposed. The exact molecular ion peak was recorded at m/z = 639.25(2.4%)(calcd. 641.86), which attributing to M^{+}+2. This appearance may base on the isotopic nature of some integral atoms as, chloride and copper-centers. Such base was supported by the appearance of two peaks at m/z = 66.09 and 63.14, which attributing to copper isotopes [33].

Scheme. 2

3.6. XRD and SEM analysis

XRD patterns were performed within the range of $10^{\circ} < 2\theta < 90^{\circ}$ (**Fig. 4 &3S**), to establish a broad view about crystal lattice dynamics of solid samples. Also, the patterns clarity reflect the purity of synthesized compounds from starting-reactants, based on referenced method [34]. All of synthesis were appeared in crystalline nanoparticle, except Cu(II)-4b complex, which appeared in amorphous morphology. Such crystalline feature, reflects the ideal packing of molecules inside the lattice, which facilitate the calculation of lattice-parameters through known relations [35]. Using FWHM method, the 2θ, d spacing, relative intensity, particle sizes, crystal strain (ε) and dislocation density (δ), were calculated and presented in Table 4. All particulate-sizes calculated, were become excellently in nanometer range, with superiority of Cu(II)-complexes than corresponding-ligands. Also, Cu(II)-complexes displayed reduced d-spacing values than the ligands, such reflects the impact of copper metals on crystal-network packing. With respect to thiazole derivatives, the values of crystal strain and dislocation density, reflect the uniformity and relatively perfect crystals of their particles. However and regarding the complexes, the values of two parameters fall within the range of ideal crystals with few imperfections which is acceptable and predictable with copper atoms. Moreover, the topography, morphology and the microstructures of all synthesis, were tested and photographed (Fig. 4S) by electron beam scanning for solid surfaces. Regarding thiazole derivatives, the particulate-features appear by high extent of similarity, which logical with fixed moieties. While and regarding Cu(II)-complexes, clear discrimination in all topographic features with that of free organic derivatives (**4a-e**), assert on purity. The spherical particulate-shape, was commonly observed, which may serve perfectly in broad spectrum of applications [36], as dyeing and antitumor-activity.

3.7. Thermogravimetric analysis

All synthesized Cu(II)-thiazole complexes were tested in this analysis aiming the confirm their suggested formulae(Fig. 5S). Also, discriminate the type of attachment for solvent-molecules towards the coordination sphere. The most fitted postulation for thermal-decomposition pathway of all TG curves, were aggregated in Table 5. All tested complexes were completely destroyed under the influence of temperature up to ≈ 900 ^{o}C, mainly in four stages. All complexes were thermally-unstable due to presence of crystal-water molecules, which easily released at low temperature (< 100 ^{o}C). Successive follower decomposition-stages, were attached with mass-loss, which apparently matching with that proposed-theoretically. All decomposition-curves reached to steady state, which attributing to the residual part, that include two copper atoms mainly as oxide.

3.8. CT-DNA binding

The degree of binding of most thiazole derivatives toward CT-DNA was studied spectrophotometry using absorption titration method. Constant concentration was taken from each derivative and then, regular increasing amounts from DNA were added at 25°C. Uv-Vis scanning curves (Fig. 6S) were obtained over fresh solutions against reference solution for each concentration (blank). Each blank solution, includes all additives except the organic amount, to remove the unwanted absorption from excess DNA out of intended binding medium. The intrinsic binding constants (K_b) for tested derivatives (all of them except H-PTAC) were estimated through an observable shift in definite charge transfer(CT) band (see figure 4S, for pointed CT band). A significant hyperchromic effect as well as a slight shift in a considered CT band(2-3nm), were observed attaching with increasing DNA amount. This feature points to the stability of binding between the ligand and DNA helix. The spectral appearance may refer to the electrostatic attraction or the occlusion of tested compound inside the minor or major grooves. Furthermore, the hyper-chromic characteristic may be explained based on the following; i) the elongated surface area for the tested compounds, which facilitate electrostatic attraction over a whole DNA helix with various spots. ii) Occlusion of tested compounds inside the grooves, led to re-organization for DNA helix. This need fractional release or damage for double helix at the surfaces phosphate, leading to the formation of cavity appropriate for entering the compound. Applying known spectral relationships [37], the binding constants (K_b, M^{-1}) were calculated and appeared as fellow; 3.92 x10^4(H-ATAC), 2.35 x10^5(H-TTAC), 4.92 x10^5(H-CTAC) and 9.64 x10^5 (H-AcTAC). This behavior agrees well with Hammett's hypothesis[38]. The relation between K_b & Hammett's constants (σR)(Fig. 5), introduces the influence of *p*-substituent on the degree of binding (K_b).

3.9. Conformational study

3.9.1. DFT/B3LYP method

The most fitted distribution for functional groups inside atomic-skeleton, was achieved for all new synthesis (Fig. 1S & 2), by applying Gaussian09 program through density function method. Two essential computed files were extracted as, log & chk. Such files were visualized over Gauss view screen according to numbering scheme. Essential information were extracted from log files and displayed in supplementary file (Table 1S). Whiles, other significant parameters (Table 6) were computed based on frontier energy gaps ($\Delta E = E_{LUMO} - E_{HOMO}$). Also, HOMO & LUMO images for all optimized structures were obtained from chk files and displayed (Figs. 6,7 & 7,8S). With respect to thiazole-derivatives, HOMO& LUMO levels were appeared elongated over a whole molecule. Such may attribute to distributed functional-groups, as well as high virtual conjugation. In addition to and regarding Cu(II)-complexes, the two levels appeared in high similarity, and centered around central atoms.

3.9.1.1. Estimated Physical parameters

Based on frontier energy gape (ΔE) and using referenced relations [23,24], electronegativity (χ), chemical potential (μ), global hardness (η), global softness (S), global electrophilicity index (ω) and absolute softness (σ) were estimated and presented (Table 6). With respect to Cu(II)-complexes and in comparing with free derivatives, we concluded the following observations;. i) The values of electrophilicity index (ω), are broadly elevated in complexes, than the corresponding derivative. Such significant index, which considered the best indicator for the degree of toxicity and reactivity, clarified the superiority of complexes. ii) The global hardness (η) and absolute softness (σ), which known as opposite indexes, their values reflect the high softness of synthesized complexes, which favor in biological activity [39,40]. The general enhancement recorded in physical characteristics of complexes, may refer to the impact of central atom on exceeding the ΔE values, which considered the indicator for advancement [41]. Other physical parameters were extracted from log files and displayed in Table 1S. Such parameters were as, bond lengths, selected atomic charges, Heat of formation (E), dipole moment (D), oscillator strength ($\int$)and excitation energies(E). The contributing donor atoms (N &O) were appeared have high negative charges, which considerably minimized after complexation. While, sulfur atom appeared as positively charged, which pushed its exclusion from coordination. The bond-lengths displayed, were selected to clarify lengthen of such bonds, after coordinating their donor side. The noticeable reduction in the formation energy of complexes, reveal their high stability comparing to

original derivatives. Also with respect to complexes, the general minimization of oscillator strength values, reflect facilitated electronic-transition inside their molecular orbital building, as the influence of metal atoms. Moreover, the lowering in dipole moment in complexes, may reflect extent of covalence, especially with the presence of chloride atoms by covalent feature [42].

3.9.1.2. Electron density maps

The density maps of all optimized structures (Fig. 8 & 9S) were established after charge distribution and building cubic surface. The electrophilic and nucelophilic attack-points, were resolute by their electrostatic potential. The atomic-colors point to their degree of electron-density. With respect to blue zone, which points to electron-poor region, which may face nucelophilic attack. While, the red zone, points to electron-rich region, which may face electrophilic attack. Additionally, green color specified to electrostatic potential region. The displayed maps supports by excellent way the ruling out of sulfur atom from coordination due to its electrophilic nature with electron-lack.

3.9.2. Molecular Docking study

To give a good impact about the antitumor behavior of our new synthesis before actual study, we interested to make such docking towards three tumor cell-lines as PDB for, 1miu, 4kg9 and 5jm5 proteins (breast, colon & liver), which will be screened actually. This aiming to investigate underlining mechanism of binding mode and affinity between tested compound and amino-acids backbone. This simulation process was performed for most new synthesis, from comparative point of view, by using MOE module (v. 2015). With respect to docked thiazole derivatives (4b-e) towards three interested proteins, we summarized the following notices as displayed in Table 7; i) the most contributing co-crystallized ligand-centers were, N2, N12, S5, 5-ring and 6-ring towards various amino acids-receptors. ii) The interaction types were covered all expected pathways as, H-π, π-π, H-donor and H-acceptor. iii) The relative mean of standard deviation were found ≤ 4.0 □. iv) The binding score values (S ≈ -6.0 kcal/mol) reflect the degree of stability of docked complexes and can be arranged as such descending order, 4d > 4c > 4b > 4e. This arrangement was based on the revers relation among them as, the degree of minimizing energy-score value, the high degree of stability for docking complexes [43]. With respect to docked co-crystallized Cu(II)-complexes towards the same proteins, we summarized the following notices as; i) the complexes were mainly bonded intensively than that of free derivative and through most possible centers (Table 7). ii) Also, the interaction types were covered all expected pathways as, H-π, π-π, H-donor and H-acceptor in addition to ionic binding. iii) The

relative mean of standard-deviation were found more lengthen than that of corresponding derivatives, which expected in coordinating compounds [44]. iv) The binding score values appeared comparable with that of corresponding derivatives with superiority of Cu(II)-CTAC,4e complex. Regarding the figures displayed (Figures 9& 10-12S), which clarify the binding centers of docked chelate with various amino acids backbones, assert the degree of interaction in simulation process. With respect to surfaces and maps (Figure 10) extracted for selected docking complexes, which assert on intensive interacting centers in Cu(II)-complexes towards the electron density over amino acids in pathogen proteins. Moreover, the docking simulation was also achieved for a reference drug (doxorubicin), for ideal comparison. The interaction net result, may push the Cu(II)-CTAC,4e complex, as a strong competitor in antitumor drug market. Finally, molecular docking study is considered the preliminary step in drug industry, which may give a good impression about the true behavior, which may be happened actually.

3.10. Successful usage of dyed- bandage for cancerous wounds

Utilizing SulphoRhodamine-B (SRB) assay, the cytotoxic impact of synthesized Cu(II)-thiazole complexes on various cell lines as, MCF-7, HCT 116 and HepG2 in addition to normal cell line (HSF), was evaluated. It was known that, the cellular-morphological changes, are commonly attached with IC_{50} values. The tested complexes displayed less significant cytotoxicity and viability reduction in a dose-response manner with very weak potential selectivity against tested different cell lines even the normal cells (Table 8 & Figs. 11&13S). Interestingly, the highest anti-proliferative cytotoxic activity of most complex, were detected against HCT116 colon cancer cell line with IC_{50} ranged from 33.6±2.82 to >1000±18. While, their impact against other cell lines, were ranged between moderate and insignificant on all cell lines even normal cells. It is worthy to note that, the screening study was conducted over pigmented cottons, to assess the extent of success, as bandage for cancerous-wounds. The cellular-behavior against dyed fibers inside the media, was varied but interesting. MCF-7 went to form colonies around fibers, the environment appears the same with HCT116 colon cancer, which was very clear indicating that, the cells are more sensitive to fibers-dye. Whereas, the same cells displayed another behavior against fibers not well dyed (Figs. 11& 13S). The most lighted point was, that the normal cells did not present any reaction against the all fiber groups (dyed or not). Furthermore, the use of fluorescent Acridine Orange (AO) and Ethidium Bromide (EtBr) mixed stain showed that cells were attached to the fibers, which indicate that the fibers are not toxic at all. Effect in a biologic system are not produced by a chemical agent unless the agent or its metabolite interact with appropriate

receptors in the system in a sufficient time and concentration. Not only that, but also many medicines are capable to be more active or may be lost their activity under the variation of body fluids conditions like pH, or they may interact with other minerals or ions. In the light of these convictions, to keep cancer cells under control, the present study suggested an innovative idea depends on the feature that the microenvironment around the colony of cancer cells is generally acidic. Moreover, the acidity condition may leads to breakdown the tight junction between cells, which may enhance the probability of metastasis. The current study aimed to produce a trap bandage act associated with the increase of pH in the microenvironment of the cancer cells colony to avoid the metastasis of released cells. Since it is easy to monitor the pH change in cell culture media, the fibers were placed at the petri dishes at the same time that the cells were cultured, to represent the model of metastatic cells. Therefore, this will keep cancer cells in low activities. This release of dye (complex), may reflect its weak attachment with the cotton fiber which already sensitive to pH value. Hence, the pigmented-bandage may contribute not to eliminate cancer, due to weak toxicity recorded, but to reduce the activity of cancer cells through regulating the pH.

4. Conclusion

New Cu(II)-thiazole complexes, were prepared and characterized using possible spectral and analytical tools. The molecular and structural formulae were proposed. The structural forms were optimized by using an advanced software, for conformation. The molecular docking was performed using MOE module against selected three cancer proteins (1miu, 4k9g & 5jm5), to establish preliminary view about the degree of inhibition for suggested drugs (synthesized compounds). A promising prediction for treated complexes to be good tumor inhibitors, pushed us for antitumor application. Such application was conducted by two ways, firstly by traditional way of application to calculate IC_{50}. Secondly and through unusual process, the screening was carried out on cotton fabrics after dyeing by these complexes, to be tested as a bandage for cancerous wounds. The results were highly satisfactory in achieving our goal.

References

[1] Ö. Şahin, Ü.Ö. Özdemir, N. Seferoğlu, Z.K. Genc, K. Kaya, B. Aydıner, S. Tekin, Z. Seferoğlu, Journal of Photochemistry & Photobiology, B: Biology 178 (2018) 428–439

[2] G.M. Ziarani, R. Moradi, T. Ahmadi, N. Lashgari, RSC Adv., 2018, 8, 12069-12103

[3] M. Maeda, Laser Dyes, Academic, New York, 1994.

[4] A. Gursoy, N. Karali, Turk. J. Chem. 27 (2003) 545–551

[5] B.Z. Kurt, I. Gazioglu, F. Sonmez, M. Kucukislamoglu, Bioorg. Chem. 59 (2015) 80–90.

[6] I.P. Ejidike, Molecules, 2018, 23, 1581-1998

[7] A.M.A.Alaghaz, H.A.Bayoumi, Y.A.Ammar, S.A.Aldhlmani, J. Mol. Struct. 2013, 1035, 383–399

[8] J.H. Al-Fahemi, A.M. Khedr, I.Althagafi, N.M. El-Metwaly, F.A. Saad, H.A. Katouah, *Applied Organometallic Chemistry*, 32 (9), e4460 (2018).

[9] B. Iftikhar, K. Javed, M.S.U. Khan, Z. Akhter, B. Mirza, V. Mckee, J. Mol. Struct. 2018, 1155, 337–348.

[10] B. Naik, K.R. Desai, Indian J. Chem. 45 (B) (2006) 267–271.

[11] E. Wong, M. Christen Giandomenico, Chem. Rev. 99 (1999) 2451–2466.

[12] A.M. Florea, D. Büsselberg, review, Cancer 3 (2011) 1351–1371.

[13] Hanadi A. Katouah, Jabir H. Al-Fahemi , Marwa G. Elghalban, Fawaz A. Saad, Ismail A. Althagafi, Nashwa M. El-Metwaly and Abdalla M. Khedr, Materials Science and Engineering: C, , 96, 740–756 (2019).

[14] I.Althagafi, N.M. El-Metwally, M.Elghalban, T.A. Farghaly, A.M. Khedr, Bioinorganic Chemistry and Applications, 2018, 1-15 (2018).

[15] B.S. Creaven, B. Duff, D.A. Egan, Inorg. Chim. Acta 2010, 363, 4048–4058.

[16] H. M. Ibrahim, S. Makhseed, R. M. Abdel-Motaleb, A. A. Makhlouf, M. H. Elnagdi. *Heterocycles*, **2007**, 71, 1951-1966.

[17] Zarkogianni Maria, Eleftheriadis Ioannis, Nikolaidis Nikolaos and Tsasaroni Eforia, *Textile Research Journal*, 9,2014

[18] M. E. Reichmann, C. A. Rice, C. A. Thomos, P. Doty, *J. Am. Chem. Soc*., 1954, 76, 3047; J. Marmur, *J. Mol. Biol*. **1961**, *3*, 208.

[19] A. Wolfe, G. H. Shimer, T. Meehan, *Biochemistry*, **1987**, *26*, 6392.

[20] A. I. Vogel. Text Book Of quantitative Inorganic Analysis Longman, London **1986.**

[21] M. J. Frisch, et al., Gaussian 09, Revision D, Gaussian, Inc., Wallingford, CT, **2010**.

[22] R. Dennington, T. Keith , J. Millam .Gauss View, Version 4.1.2, SemichemInc, Shawnee Mission, KS, **2007**.

U. El-Ayaan, N. M. El-Metwally, M. M.Youssef, S. A. A. El Bialy, *Spectrochim. Acta, Part A,*

[23] **2007**, *68*, 1278.

[24] R. K. Ray, G. R. Kauffman, *Inorg. Chem. Acta*, **1990**, *173*, 207.

[25] Khlood H. Mashat , Bandar A. Babgi, Mostafa A. Hussien, Polyhedron 158 (2019) 164–172

[26] Gamil A. Al-Hazmi, Khlood S. Abou-Melha, Nashwa M. El-Metwaly and Kamel A. Saleh, Bioinorganic Chemistry and Applications, 2018, Article ID 7176040, 22 pages

[27] W.J. Geary, Coord. Chem. Rev. 7 (1971) 81-122.

[28] A.M. Khedr, D.F. Draz, J. Coord. Chem., 63 (8), 1418–1429 (2010).

[29] K.S. Abu-Melhaa, N.M. El-Metwally, Spectrochim. Acta A 70 (2008) 277–283.

[30] A.A. Abou-Hussen, N.M. El-Metwaly, E.M. Saad, A.A. El-Asmy, J. Coord. Chem. 58 (2005) 1735-1749.

[31] A.M. Khedr, S. Jadon, V. Kumar, J. Coord. Chem., 64, 1351–1359 (2011).

[32] A. B. P. Lever, Inorganic Electronic Spectroscopy, Elsevier, Amsterdam 1986.

[33] M. S. Refat, N. M. El-Metwaly, *Spectrochimica Acta Part A*, **2011**, *81*, 215.

[34] B. D. Cullity, Elements of X –ray diffraction. Second ed., Addison –Wesley Inc., **1993**.

[35] S. Velumani, X. Mathew, P.J. Sebastian, Sa.K. Narayandass, D. Mangalaraj, *Sol. Cells*, **2003,** *76*, 347.

[36] J. S. Ritch, T. Chivers, K. Ahmad, M. Afzaal, P. O. Brien, *Inorg. Chem*., **2010**, *49*, 1198; T. Mokari, M. Zhang, P. Yang, *J. Am. Chem. Soc*. **2007**, *129*, 9864; J. J. Urban, D. V. Talapin, E. V. Shevchenko, C. B. Murray, *J. Am. Chem. Soc*., **2006,** *128*, 3248.

[37] A.Z. El-Sonbati, A.F. Shoair, A.A. El-Bindary , M.A. Diab, A.S. Mohamed, *J. Mol. Liq*., **2015**, *209*, 635

[38] L. H. Abdel-Rahman, A. M. Abu-Dief, N. M. Ismail, M. Ismael, *J. Inorg.Nano-Metal Chem*. **2017**, *47*, 467

[39] R. C. Chikate, S. B. padhye, *Polyhedron*, **2005**, *24*, 1689.

[40] S.Sagdinc, B.Köksoy, K.F.andemirli, S.H. Bayari, *J. Mol. Struct*., **2009**, *917*, 63.

[41] I. Fleming, Frontier Orbital's and Organic Chemical Reactions, Wiley, London, **1976**.

[42] S. K.Tripathi,R.Muttineni, S. K. Singh, *J. Theor. Biol.*, **2013**, *334*, 87.

[43] Ahmed A. Fadda, Ehab Abdel-Latif,* Ahmed Fekri, and Amal R. Mostafa, *J. Heterocyclic Chem.*, **00,** 00 (2019).

[44] Somaia S. Abd El-Karima, Manal M. Anwara, Yasmin M. Syama, Manal A. Naelb, Hanan F. Alia, Mohamed A. Motaleb, Bioorganic Chemistry 81 (2018) 481–493

[45] C. Fosset, B. A. McGaw, and M. D. Reid, Journal of Inorganic Biochemistry, vol. 99, no. 5, pp. 1018–1022, 2005

[46] Gamil A. Al-Hazmi, Khlood S. Abou-Melha, Nashwa M. El-Metwaly and Kamel A. Saleh, Bioinorganic Chemistry and Applications, Volume 2018, Article ID 7176040, 22 pages

Table 1. Analytical characteristics for synthesized Cu(II)-thiazole complexes

Compounds (Empirical formula)	Λ_m, $Ohm^{-1}cm^2 mol^{-1}$	Color	Elemental analysis (%) Calcd (Found)					
			C	H	N	S	Cu	Cl
1)($C_{12}H_9N_5OS$)(H-PTAC,**4a**)(271.30)	---	Orange	53.13(53.13)	3.34(3.33)	25.81(25.80)	11.82(11.80)	-----	------
2)[Cu_2Cl_3(PTAC)(H_2O)]H_2O(539.77)	5.12	Olive green	26.70(26.65)	2.24(2.24)	12.97(12.97)	5.94(5.92)	23.55(23.56)	19.70(19.71)
3)($C_{13}H_{11}N_5OS$)(H-TTAC,**4b**)(285.33)	---	Golden	54.72(54.70)	3.88(3.85)	24.55(24.53)	11.24(11.22)	------	-----
4)[Cu_2Cl_3(TTAC)(H_2O)$_4$]2H_2O(625.86)	---	Brown	24.95(24.94)	3.54(3.55)	11.19(11.18)	5.12(5.13)	20.31(20.31)	16.99(17.03)
5)($C_{13}H_{11}N_5O_2S$)(H-ATAC,**4c**)(301.33)	---	Golden	51.82(51.80)	3.68(3.67)	23.24(23.24)	10.64(10.65)	------	------
6)[Cu_2Cl_3(ATAC)(H_2O)$_4$]2H_2O(641.86)	---	Brownish yellow	24.33(24.31)	3.45(3.44)	10.91(10.90)	5.00(5.01)	19.81(19.81)	16.57(16.55)
7)($C_{14}H_{11}N_5O_2S$)(H-AcTAC,**4d**)(313.34)	---	Violet	53.67(53.66)	3.54(3.52)	22.35(22.33)	10.23(10.27)	-----	------
8)[Cu_2Cl_3(AcTAC)(H_2O)]H_2O(581.81)	6.82	Olive green	28.90(28.92)	2.43(2.44)	12.04(12.02)	5.51(5.49)	21.84(21.88)	18.28(18.30)
9)($C_{12}H_8ClN_5OS$)(H-CTAC,**4e**)(305.75)	---	Red	47.14(47.15)	2.64(2.64)	22.91(22.91)	10.49(10.48)	------	------
10)[Cu_2Cl_2(CTAC)(H_2O)$_2$]Cl.H_2O(592.24)	55.19	Olive green	24.34(24.33)	2.38(2.37)	11.82(11.81)	5.41(5.41)	21.46(21.46)	23.94(23.95)

Table 2. Functional IR spectral bands (cm^{-1}) for thiazole derivatives (4a-e) and their Cu(II) complexes

Compounds	νOH,νNHs	νC=O	νC=N	νC-S	νC-O	νCN	δNHs	δr(H_2O), δw(H_2O)	νM-O	νM-N
1)($C_{12}H_9N_5OS$)(H-PTAC,**4a**)	3420,3215,3150	1690	1633, 1594	670	1093	2217	1534, 1554			
2)[Cu_2Cl_3(PTAC)(H_2O)]H_2O	3430,3174	----	1616,1605	677	1078	2219	1534	860, 691	570	492
3)($C_{13}H_{11}N_5OS$)(H-TTAC,**4b**)	3457,3228,3197	1691	1636,1602	720	1160	2220	1585, 1561	-----	----	
4)[Cu_2Cl_3(TTAC)(H_2O)$_4$]2H_2O	B.C.at 3460, 3230	----	1620, 1594	719	1137	2225	1588	854, 676	572	505
5)($C_{13}H_{11}N_5O_2S$)(H-ATAC,**4c**)	3431,3296,3187	1652	1623, 1590	696	1091	2206	1580, 1526	-----	----	
6)[Cu_2Cl_3(ATAC)(H_2O)$_4$]2H_2O	B.C. at 3452, 3170	----	1610, 1578	690	1082	2210	1530	841, 682	566	490
7)($C_{14}H_{11}N_5O_2S$)(H-AcTAC,**4d**)	3460, 3219, 3176	1688	1650,1610	671	1089	2210	1590, 1553	----	----	
8)[Cu_2Cl_3(AcTAC)(H_2O)]H_2O	3465, 3190	---	1641, 1593	681	1070	2221	1555	823, 675	571	506
9)($C_{12}H_8ClN_5OS$)(H-CTAC,**4e**)	3428, 3240,3181	1689	1655,1601	678	1090	2220	1580, 1543	----	----	
10)[Cu_2Cl_2(CTAC)(H_2O)$_2$]Cl.H_2O	3445, 3192	----	1646, 1590	688	1081	2230	1560	812, 681	578	492

B. c. Broad centered

Table 3. Electronic transition bands (cm^{-1}) for 10^{-4}M thiazole derivatives (**4a-e**) and their Cu(II) complexes

Compounds	**μ(eff) (B.M.)**	**ε_1**	**$\int$ (10^5)**	**d-d transition bands (cm^{-1}) υ_2 ; υ_1**	**Intraligand and charge transfer(cm^{-1})**	**Complex Geometry**
1)(H-PTAC,**4a**)	-----	6120	450.4	------	35,471; 30,123; 28,71, 25,501	------
2)$[Cu_2Cl_3(PTAC)(H_2O)]H_2O$	1.63	8000	588.8	18,671; 16,512	35,510; 32,831; 30.045; 25,421	Square-planer
3)(H-TTAC,**4b**)	-----	4120	473.8	------	37,120; 35,184; 32,160; 30,178	------
4)$[Cu_2Cl_3(TTAC)(H_2O)_4]2H_2O$	1.63	-----	-----	21,218; 18,821	36,459; 33,843; 31,671; 29,542	Octahedral
5)(H-ATAC,**4c**)	-----	3890	511.3	------	36,910; 35,083; 33, 120; 29,720	------
6)$[Cu_2Cl_3(ATAC)(H_2O)_4]2H_2O$	1.68	-----	-----	22,451 ;19,193	36,751; 34,821; 32,845; 29,651	Octahedral
7)(H-AcTAC,**4d**)	------	11,912	9123.3	------	36,124; 33,842; 30,348; 27,180; 22,910	------
8)$[Cu_2Cl_3(AcTAC)(H_2O)]H_2O$	1.60	15,120	11580.3	18,326; 16,521	36,032; 33,671; 30,219; 26,821	Square-planer
9)(H-CTAC,**4e**)	----	5120	606.8	------	36,032; 34,910; 31,561; 28, 900; 24,029	------
10)$[Cu_2Cl_2(CTAC)(H_2O)_2]Cl.H_2O$	1.62	5520	630.5	18,056; 16,452	35,751; 34,610; 30,871; 27,810	Square-planer

ε, Molar absorptivity. ∫ , Oscillator strengths, ∫, calculated using the following expression: ∫=4.6×10−9 εmax υ1/2, where; εmax is the molar absorptivity of the band maximum and υ1/2 is the band width at half-height expressed in wave numbers: C. J. Ballahusen, Prog. Inorg. Chem. 2.251(1960).

Table 4. XRD data for nano-crystalline compounds

Compounds	**Size (Å)**	**2θ**	**Intensity**	**d-spacing (Å)**	**ε**	**δ($Å^{-2}$)**	**FWHM**
1)(H-PTAC,**4a**)	2.8611	31.72	408	2.8186	0.1178	0.1222	0.5263
2)$[Cu_2Cl_3(PTAC)(H_2O)]H_2O$	0.9412	25.94	238	3.4321	0.4377	1.1288	1.5789
3)(H-TTAC,**4b**)	1.8811	25.62	146	3.4742	0.2216	0.2826	0.7895
4)(H-ATAC,**4c**)	2.3541	26.20	420	3.3986	0.1733	0.1804	0.6316
5)$[Cu_2Cl_3(ATAC)(H_2O)_4]2H_2O$	0.6757	32.36	226	2.7644	0.4944	2.1902	2.2316
6)(H-AcTAC,**4d**)	2.8591	31.76	226	2.8152	0.1182	0.1223	0.5266
7)$[Cu_2Cl_3(AcTAC)(H_2O)]H_2O$	0.8221	32.62	392	2.7429	0.4007	1.4796	1.8353
8)(H-CTAC,**4e**)	1.4130	26.36	408	3.3783	0.28697	0.5009	1.0526
9)$[Cu_2Cl_2(CTAC)(H_2O)_2]Cl.H_2O$	0.9245	32.50	364	2.7527	0.3574	1.1700	1.6316

Table 5. Decomposition assumption for Cu(II)-thiazole complexes

Compounds	Steps	Temp. range (°C)	Decomposed	Weight loss; Calcd(Found %)
$[Cu_2Cl_3(PTAC)(H_2O)]H_2O$	1st	25.97- 178.91	$-2H_2O+0.5Cl_2$	13.24(13.25)
	2ed	180.12- 310.72	$-Cl_2+HCN$	18.14(18.11)
	3rd	311.2- 561.96	$-C_3H_2N_2S$	18.18(18.18)
	4th	562.01- 850.41	$-C_8H_5N_2$	23.93(23.96)
	residue		CuO+Cu	26.51(26.50)
$[Cu_2Cl_3(TTAC)(H_2O)_4]2H_2O$	1st	33.97- 194.01	$-2H_2O+HCN$	10.08(10.05)
	2ed	195.22- 366.20	$-Cl_2+4H_2O$	22.84(22.82)
	3rd	367.15- 589.66	$-0.5Cl_2+C_4H_2N_2$	18.14(18.15)
	4th	590.17- 866.61	$-C_8H_7N_2$	20.96(21.01)
	residue		CuO+CuS	27.99(27.97)
$[Cu_2Cl_3(ATAC)(H_2O)_4]2H_2O$	1st	37.31- 105.21	$-2H_2O$	5.61(5.62)
	2ed	106.81- 331.76	$-1.5Cl_2+4H_2O+HCN$	32.01(32.04)
	3rd	332.11- 546.81	$-C_9H_7N_2$	22.31(22.33)
	4th	547.10- 854.90	$-C_3H_2N_2S$	15.29(15.27)
	residue		2[CuO]	24.79(24.74)
$[Cu_2Cl_3(AcTAC)(H_2O)]H_2O$	1st	45.26- 185.05	$-2H_2O+Cl_2$	18.38(18.39)
	2ed	186.11- 490.32	$-0.5Cl_2+HCN$	10.74(10.72)
	3rd	491.05- 774.91	$-C_8H_9N_4S$	33.22(33.22)
	residue		5C+2[CuO]	37.67(37.67)
$[Cu_2Cl_2(CTAC)(H_2O)_2]Cl.H_2O$	1st	28.91-97.83	$-H_2O+0.5Cl_2$	9.03(9.00)
	2ed	98.51- 237.76	$-Cl_2+2H_2O+HCN$	22.62(22.61)
	3rd	238.07- 480.60	$-C_4H_2N_2S$	18.60(18.58)
	4th	481.10- 789.61	$-C_4H_4N_2Cl$	19.51(19.57)
	residue		3C+Cu+CuO	30.25(30.24)

Table 6. Computed parameters (ev) for all optimized structures in ethanol solvent using DFT/B3LYP method

Compound	E_H	E_L	E_H - E_L	E_l-E_h	*x*	μ	η	S(eV-1)	ω	σ
4a, H-PTAC	-0.22953	-0.08618	-0.1434	0.14335	0.157855	-0.15786	0.071675	0.035838	0.173828	13.95186606
Cu(II)-PTAC	-0.23424	-0.2009	-0.0333	0.03334	0.21757	-0.21757	0.01667	0.008335	1.419817	59.9880024
4b, H-TTAC	-0.22288	-0.08464	-0.1382	0.13824	0.15376	-0.15376	0.06912	0.03456	0.171022	14.46759259
Cu(II)-TTAC	-0.15692	-0.12078	-0.0361	0.03614	0.13885	-0.13885	0.01807	0.009035	0.533462	55.34034311
4c, H-ATAC	-0.22463	-0.08629	-0.1383	0.13834	0.15546	-0.15546	0.06917	0.034585	0.174699	14.4571346
Cu(II)-ATAC	-0.23763	-0.21906	-0.0186	0.01857	0.228345	-0.22835	0.009285	0.004643	2.807832	107.7005924
4d, H-AcTAC	-0.23463	-0.09219	-0.1424	0.14244	0.16341	-0.16341	0.07122	0.03561	0.187467	14.04099972
Cu(II)-AcTAC	-0.23254	-0.19723	-0.0353	0.03531	0.214885	-0.21489	0.017655	0.008828	1.307719	56.64117814
4e, H-CTAC	-0.22929	-0.08898	-0.1403	0.14031	0.159135	-0.15914	0.070155	0.035078	0.180486	14.25415152
Cu(II)-CTAC	-0.20404	-0.14269	-0.0614	0.06135	0.173365	-0.17337	0.030675	0.015338	0.489901	32.599837

Table 7. The energy score and interaction data for most compounds against, breast, colon and liver cancers proteins

Compound	Protein	Ligand	Receptor	Interaction	Distance	E(Kcal/ mol)	S(energy score)
4b, H-TTAC	1miu	N 13	O VAL 2967 (A)	H-donor	2.96	-5.3	-5.5643
	4k9g	N 12	N PRO 1 (B)	H-acceptor	3.33	-0.5	-5.2706
		N 6	6-ring PHE 113 (B)	H- π	4.19	-0.6	
		5-ring	6-ring TYR 36 (B)	π- π	3.45	0.0	
	5jm5	N 2	N LYS 270 (B)	H-acceptor	3.05	-0.9	-6.1201
		N 12	N TYR 24 (B)	H- acceptor	3.58	-1.7	
		5-ring	CA SER 217 (B)	π-H	4.10	-0.8	
		6-ring	6-ring TYR 24 (B)	π- π	3.96	0.0	
Cu(II)-TTAC	1miu	N 15	OD1 ASP 41 (B)	H-donor	3.28	-1.4	-6.3179
		O 25	OE2 GLU 40 (B)	H- donor	2.70	-5.6	
		O 46	OD1 ASP 41 (B)	ionic	2.84	-5.6	
		O 49	OE1 GLU 40 (B)	ionic	3.12	-3.7	
	4k9g	O 49	OD1 ASN 109 (C)	H-donor	2.74	-3.5	-5.3831
		N 14	CE LYS 77 (A)	H-acceptor	3.84	-0.5	
	5jm5	N 15	OE1 GLU 237 (A)	H-donor	3.05	-6.2	-5.4438
		O 49	OE1 GLU 237 (A)	H- donor	2.94	-4.8	
		O 25	OE1 GLU 237 (A)	ionic	3.88	-0.7	
		6-ring	CD PRO 239 (A)	π-H	4.58	-0.5	
4c, H-ATAC	1miu	5-ring	CA GLN 2985 (A)	π-H	3.70	-0.8	-6.3173
	4k9g	N 2	ND2 ASN 97 (C)	H-acceptor	3.20	-0.5	-6.7481
		5-ring	CB SER 60 (C)	π-H	3.71	-0.6	
	5jm5	N 12	N LYS 270 (A)	H-acceptor	3.33	-1.0	-6.372
		5-ring	CB SER 221 (A)	π-H	3.79	-1.4	
Cu(II)-ATAC	1miu	CL 40	OE1 GLU 2641 (A)	H-donor	3.68	-0.5	-5.6385
		O 53	OD1 ASP 2613 (A)	H-donor	3.10	-1.9	
		N 2	OE1 GLU 2479 (A)	Ionic	3.62	-1.5	
		O 47	OE1 GLU 2479 (A)	ionic	2.89	-1.5	
	4k9g	6-ring	NE ARG 11 (A)	π- cation	4.21	-0.7	-4.9503
	5jm5	O 50	O GLU 237 (A)	H-donor	2.80	-15.0	-5.3137
		N 15	OH TYR 196 (A)	H-acceptor	3.25	-2.4	
		6-ring	N CYS 7 (B)	π-H	4.63	-0.7	
4d, H-AcTAC	1miu	S 5	OD2 ASP 41 (B)	H-donor	4.11	-0.9	-5.0058
		6-ring	NH1 ARG 2926 (A)	π -cation	4.36	-1.0	
	4k9g	S 5	OG SER 60 (C)	H-donor	3.20	-1.3	-6.4142
		N 11	NE2 HIS 62 (A)	H-acceptor	3.09	-0.8	
		N 12	CB SER 60 (B)	H- acceptor	3.67	-0.5	
	5jm5	N 2	ND2 ASN 280 (B)	H-acceptor	3.42	-1.2	-6.3778
		N 12	NZ LYS 270 (B)	H- acceptor	3.12	-1.7	
		5-ring	CD1 LEU 219 (B)	π-H	3.92	-0.5	
		6-ring	CB LYS 270 (B)	π-H	3.78	-0.6	
Cu(II)-AcTAC	1miu	O 45	OE1 GLU 2824 (A)	Ionic	2.95	-7.8	-5.5061
		6-ring	5-ring HIS 2817 (A)	π- π	3.77	-0.0	
	4k9g	O 26	N PRO 1 (B)	H-acceptor	2.94	-4.8	-5.8605
	5jm5	N 13	O ASP 156 (B)	H-donor	3.09	-7.5	-5.5401
		N 15	CA LYS 136 (A)	H-acceptor	3.56	-0.8	
		O 26	NH1 ARG 96 (B)	H- acceptor	2.97	-2.2	
		6-ring	CB ASN 134 (A)	π-H	3.14	-0.8	
		6-ring	CA ALA 157 (B)	π-H	3.19	-0.5	
4e, H-CTAC	1miu	C 15	5-ring HIS 2791 (A)	H- π	3.96	-0.7	-4.9259

	4k9g	N 12	N PRO 1 (B)	H-acceptor	3.24	-6.4	-5.0639
	5jm5	------	------	------	------	------	-5.8681
Cu(II)-CTAC	1miu	N 13	OD2 ASP 41 (B)	H-donor	3.21	-10.3	-5.6783
		N 16	OE2 GLU 40 (B)	H-donor	3.06	-2.3	
		O 40	OE2 GLU 40 (B)	H-donor	2.70	-2.6	
		O 40	OE2 GLU 40 (B)	ionic	2.70	-6.9	
	4k9g	C 4	O ALA 114 (A)	H-donor	3.26	-0.5	-4.4128
		N 13	OG SER 111 (A)	H-donor	3.41	-1.1	
		O 43	O ALA 114 (A)	H-donor	2.74	-20.9	
		N 2	O ALA 114 (A)	ionic	3.87	-0.8	
		O 43	OXT ALA 114 (A)	Ionic	3.48	-2.0	
	5jm5	N 7	OD1 ASN 307 (B)	H-donor	3.37	-2.0	-5.0724
		CL 36	O HIS 304 (B)	H-donor	3.25	-0.5	
		O 43	OD1 ASP 309 (B)	H-donor	2.75	-18.2	
		O 43	OD1 ASP 309 (B)	ionic	2.75	-6.4	
Doxorubicin	1miu	O 19	CA GLY 3059 (A)	H-acceptor	3.42	-0.5	-6.5117
		O 29	NH1 ARG 2893 (A)	H- acceptor	2.97	-3.0	
		O 38	NZ LYS 2891 (A)	H- acceptor	3.46	-1.1	
		6-ring	N HIS 3060 (A)	π-H	4.69	-0.5	
	4k9g	------	------	------	------	------	-5.2151
	5jm5	O 29	OD2 ASP 109 (A)	H-donor	2.86	-1.2	-5.7434
		O 19	NE ARG 66 (A)	H- acceptor	3.05	-1.3	

Table 8: The IC_{50} (µg/ml) of different complexes against different solid tumor cell lines (HCT116, MCF-7, HepG-2) and HSF as a normal cell line.

Item	**HCT-116**	**MCF-7**	**HepG-2**	**HSF**
Cu(II)-4a	>100±0.43	>300±2.21	>300±0.90	>1000±1.67
Cu(II)-4b	>1000±0.18	>300±0.97	>600±1.85	>200±2.43
Cu(II)-4c	46.15±2.48	>1000±1.84	>400±1.58	>300±1.47
Cu(II)-4d	63.11±1.96	>300±1.84	>500±1.52	>200±0.85
Cu(II)-4e	33.6±2.82	>200±0.51	>200±1.63	>200±1.33
Doxorubicin	0.3979±0.052	0.6025± 0.02	0.3428± 0.10	0.831± 0.21

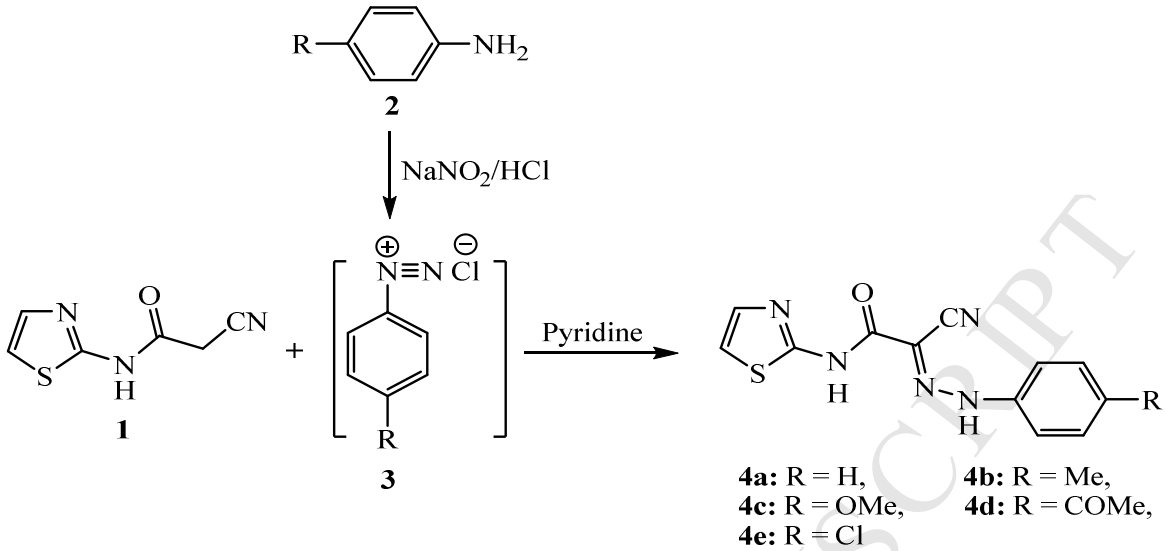

Scheme. 1. Synthesis procedure of *N*-aryl-2-oxo-2-(thiazol-2-ylamino)-acetohydrazonoyl cyanide derivatives 4a-e

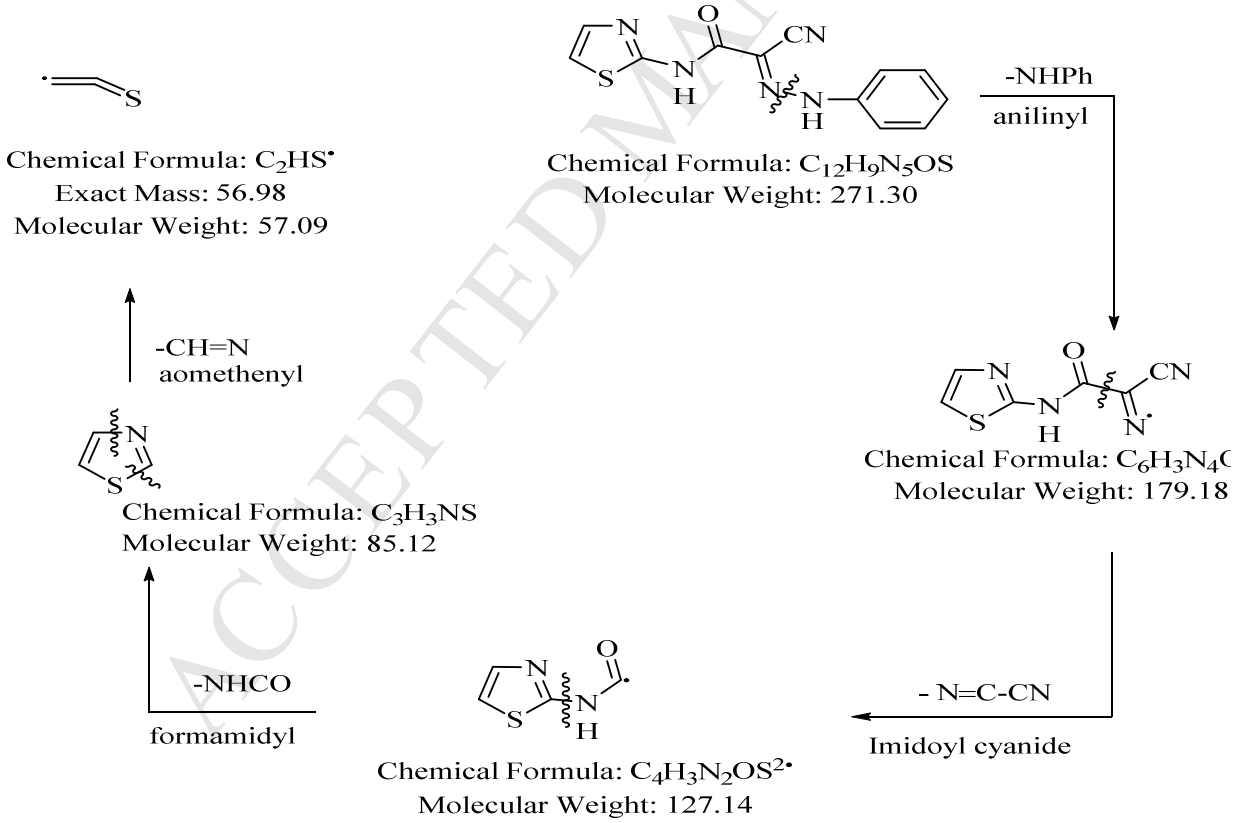

Scheme. 2. The fragmentation pattern of thiazole derivative (4a, H-PTAC)

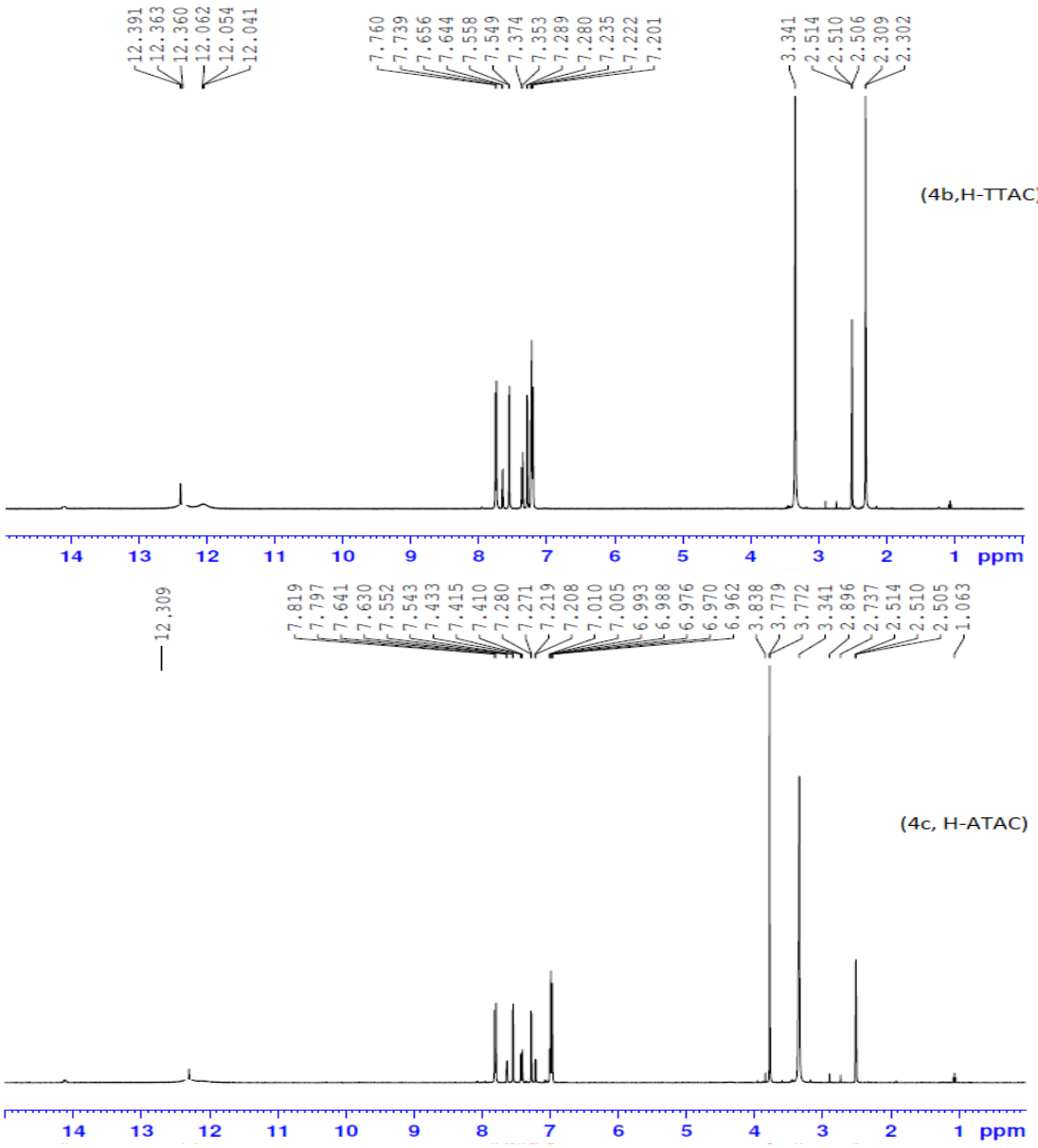

Fig.1 . ^{1}H NMR spectra of two chosen thiazole derivatives

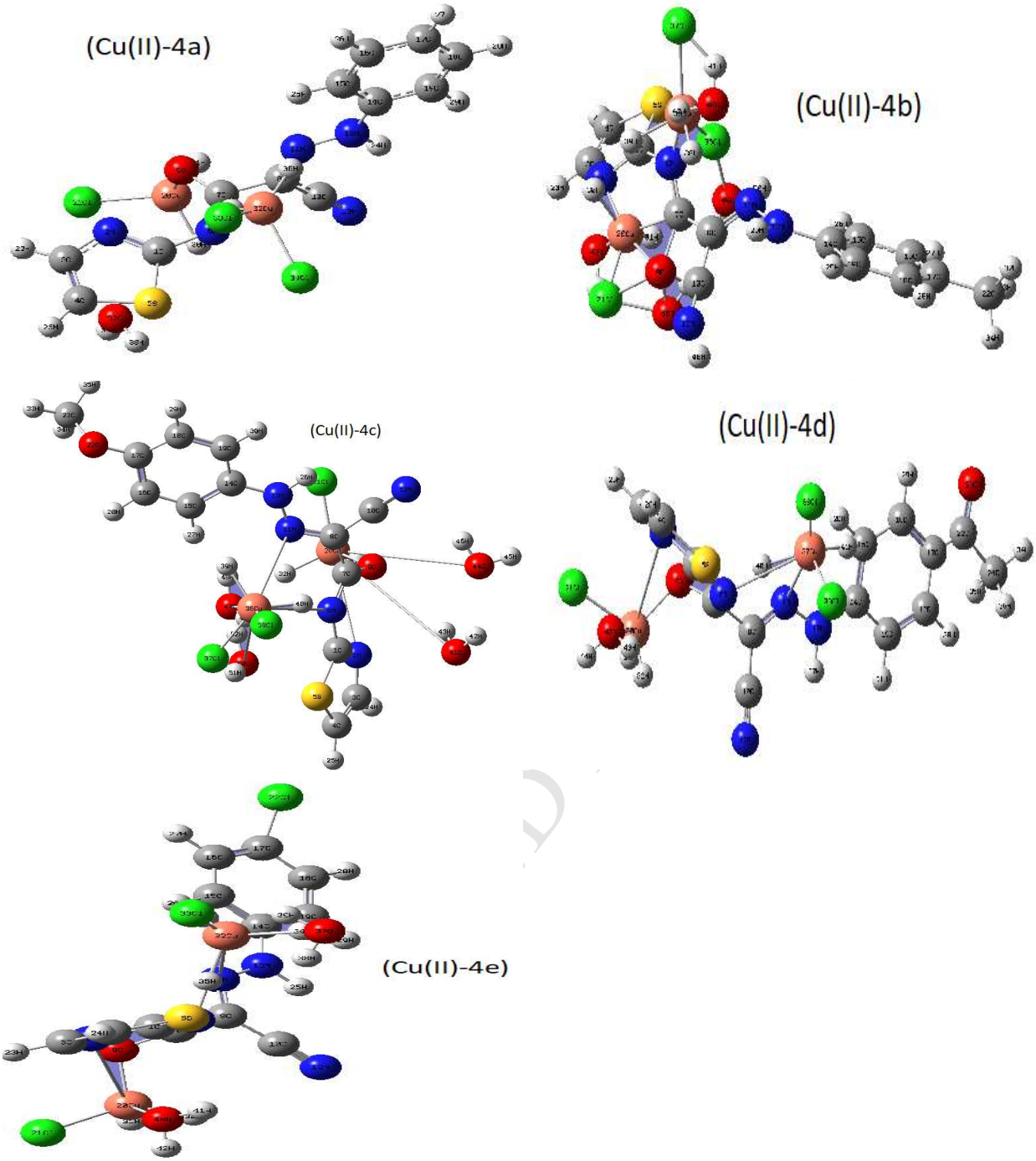

Fig. 2. Optimized structures of Cu(II)-thiazole complexes

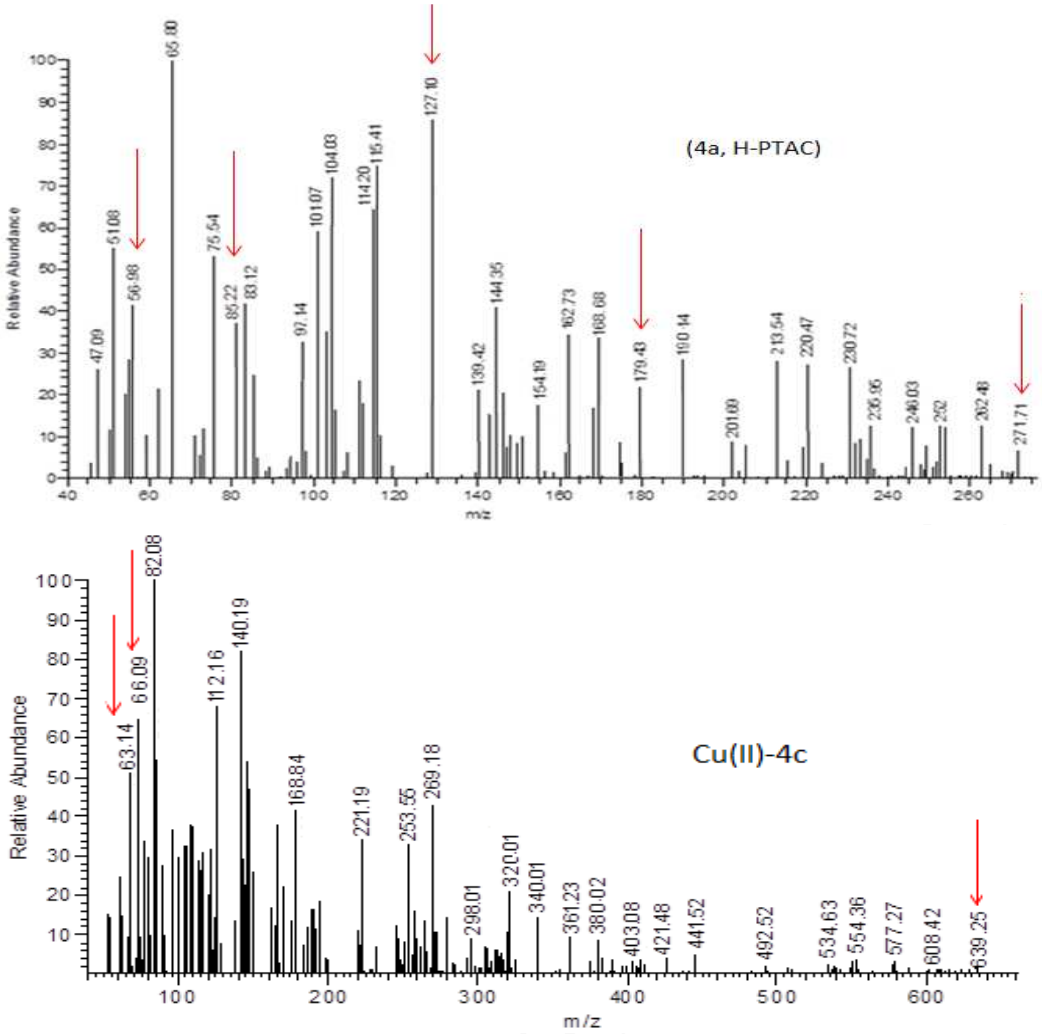

Fig. 3. Mass spectra of two selected compounds

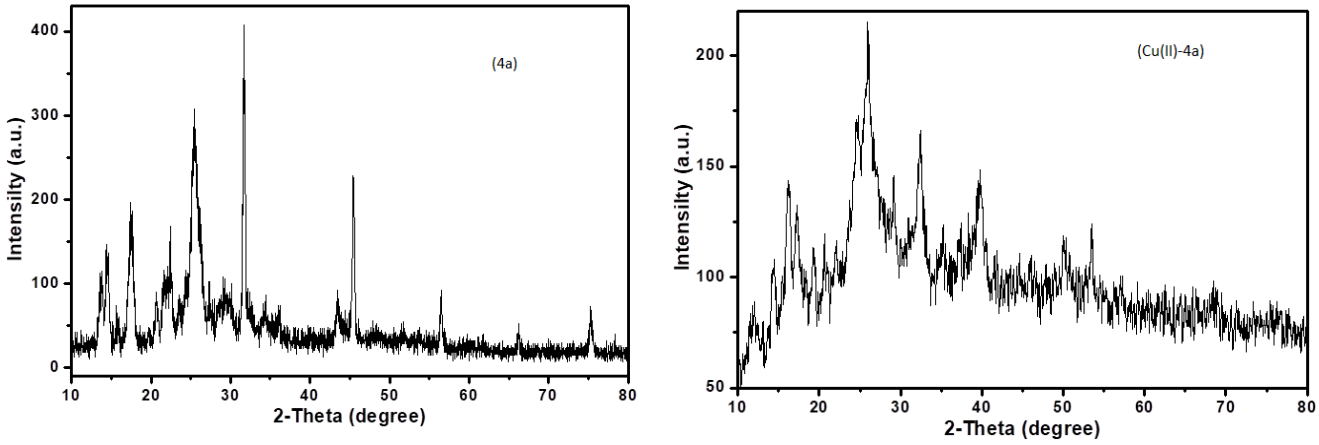

Fig. 4. XRD patterns for nano-crystalline 4a, H-PTAC derivative and its Cu(II) complex

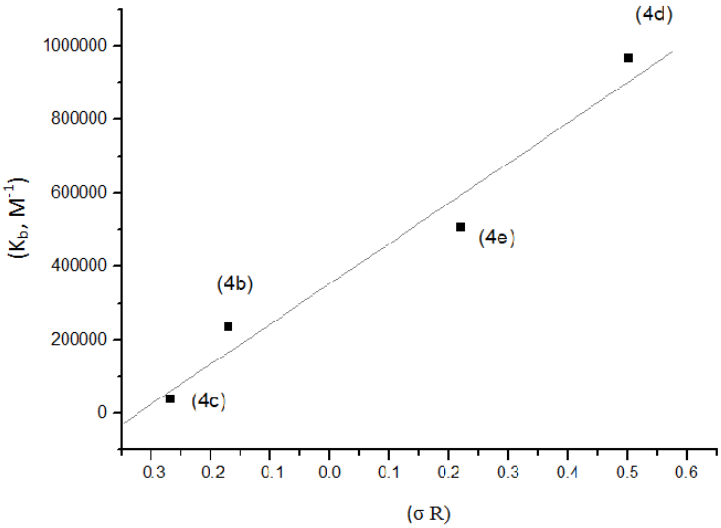

Fig. 5 . Hammett's relation between p- substituent (σ R) values vs intrinsic binding constants (Kb) of triazole derivatives.

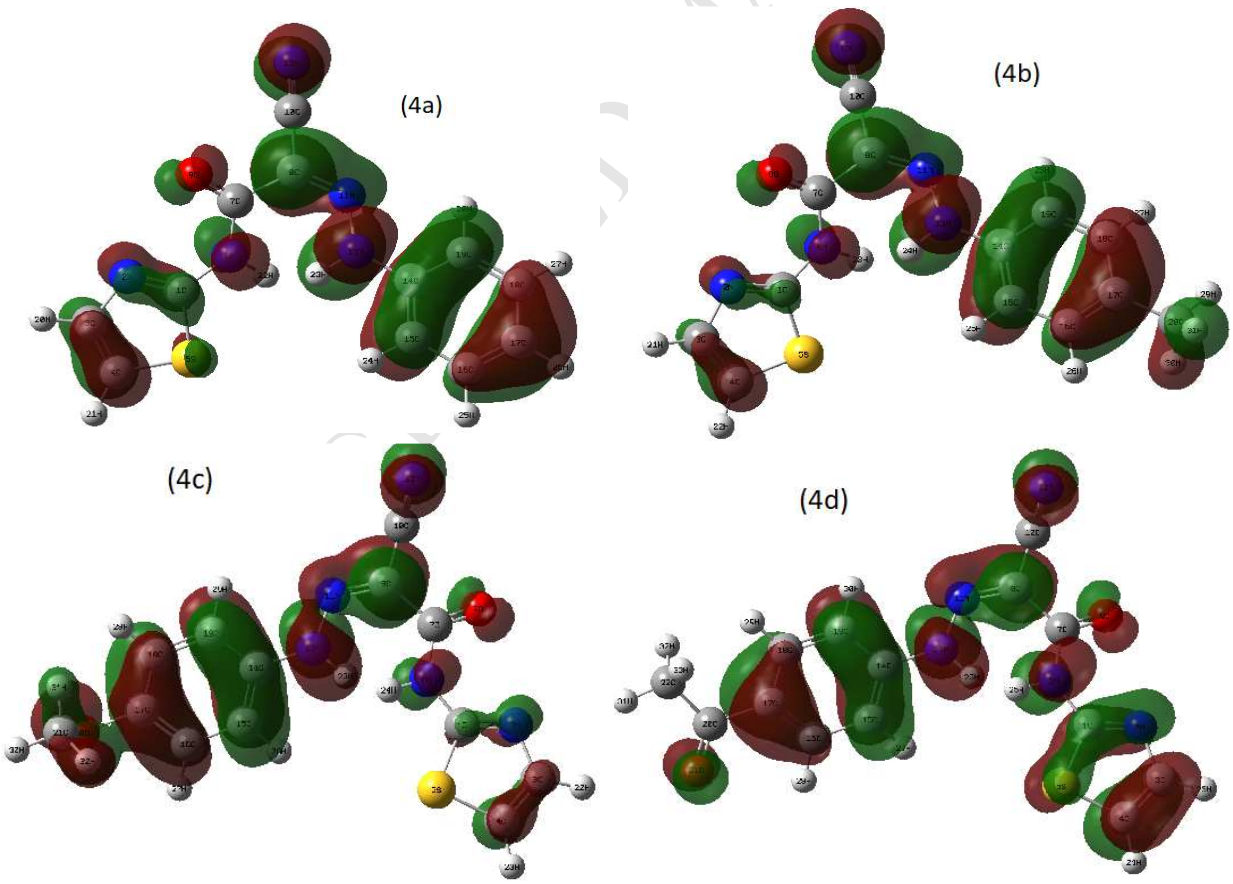

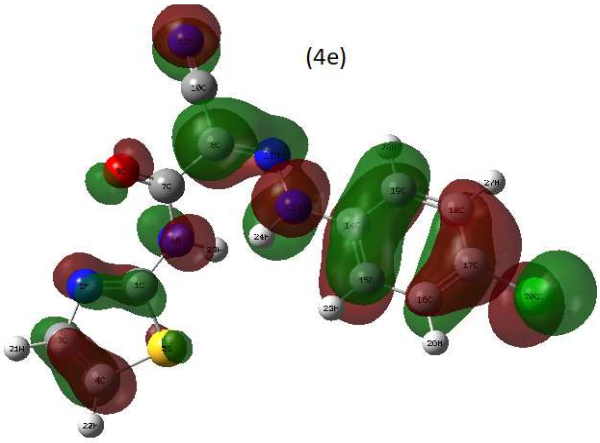

Fig.6 . Frontier HOMO images of enol- form of thiazole derivatives

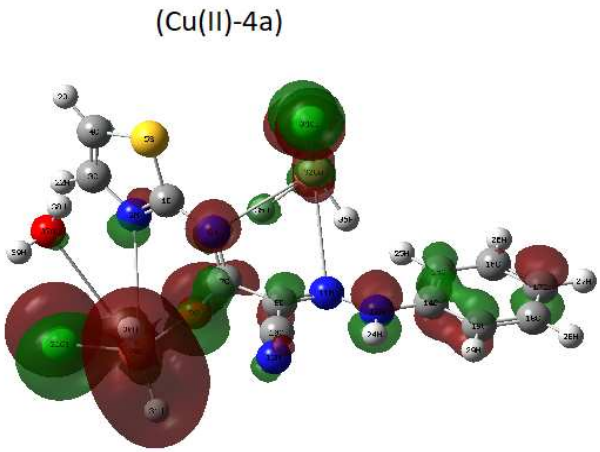

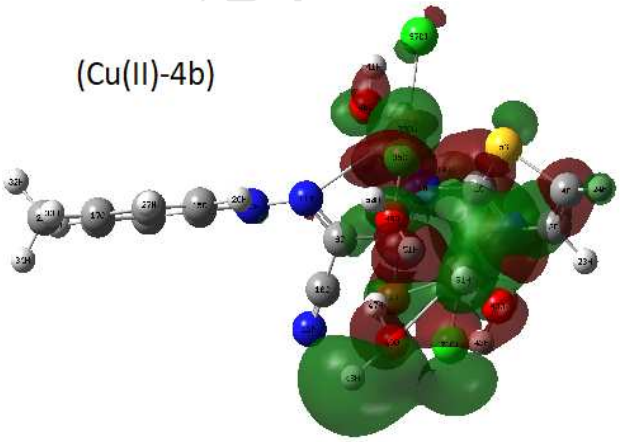

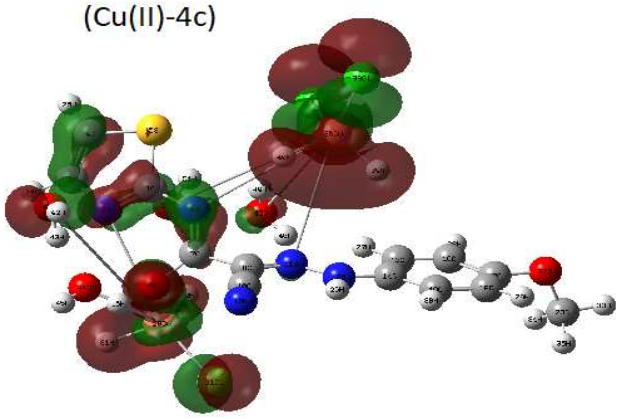

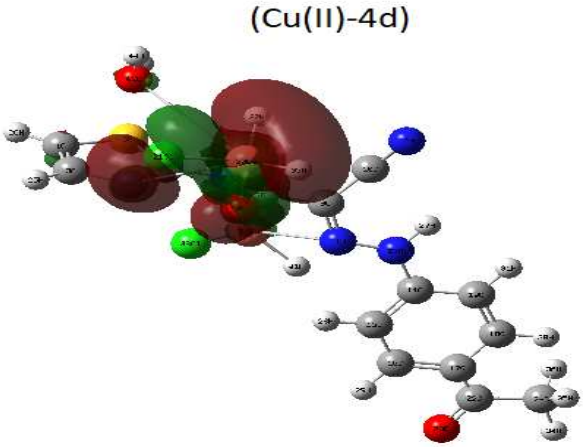

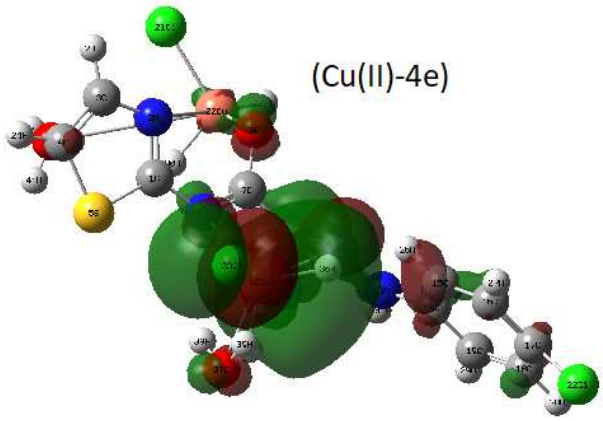

Fig. 7. Frontier HOMO images of Cu(II)-thiazole complexes

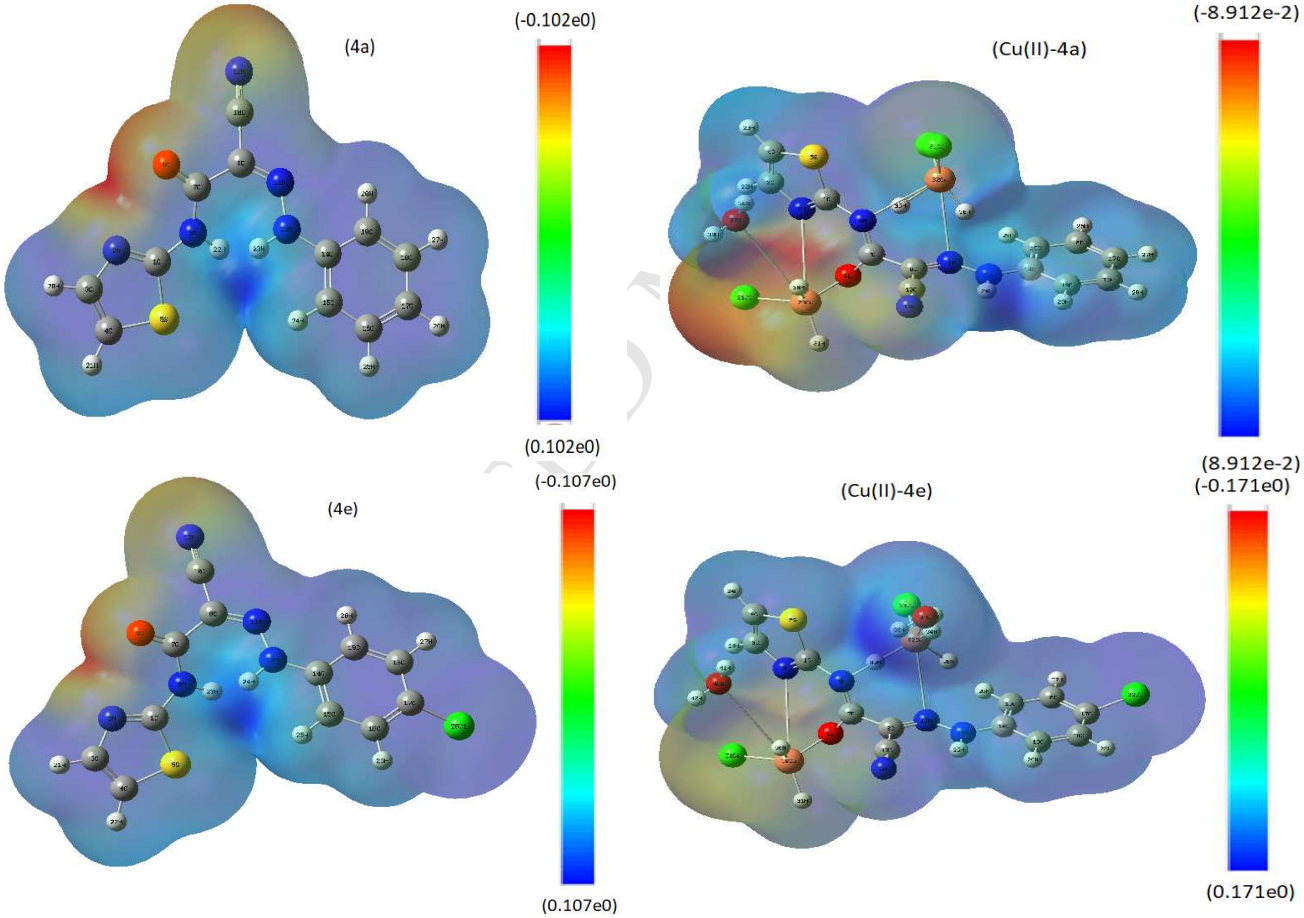

Fig. 8 . Electron density maps of 4a, H-PTAC & 4e- CTAC derivatives and their Cu(II) complex

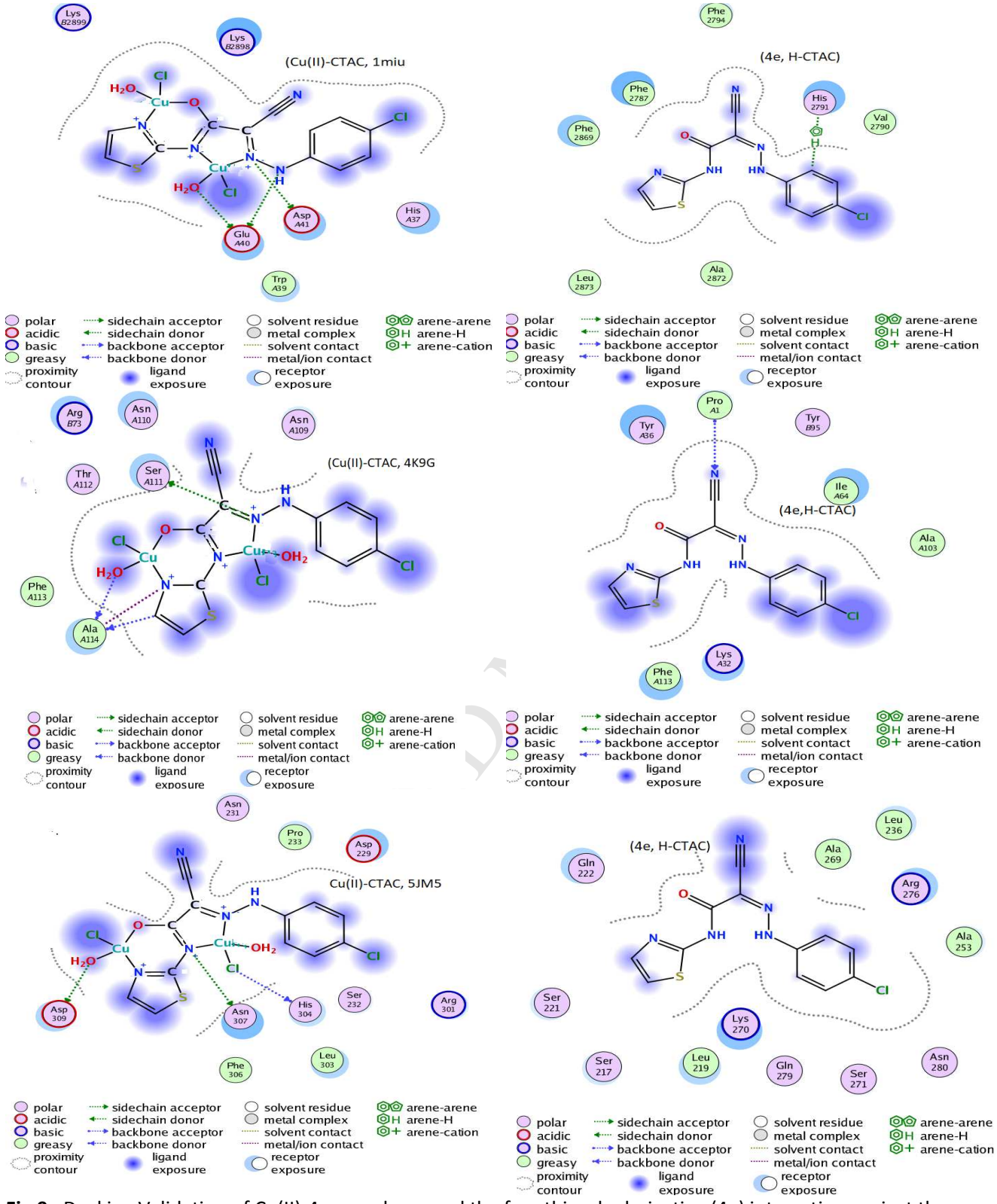

Fig.9. Docking Validation of Cu(II)-4e complexes and the free thiazole derivative (4e) interaction against three cancer proteins

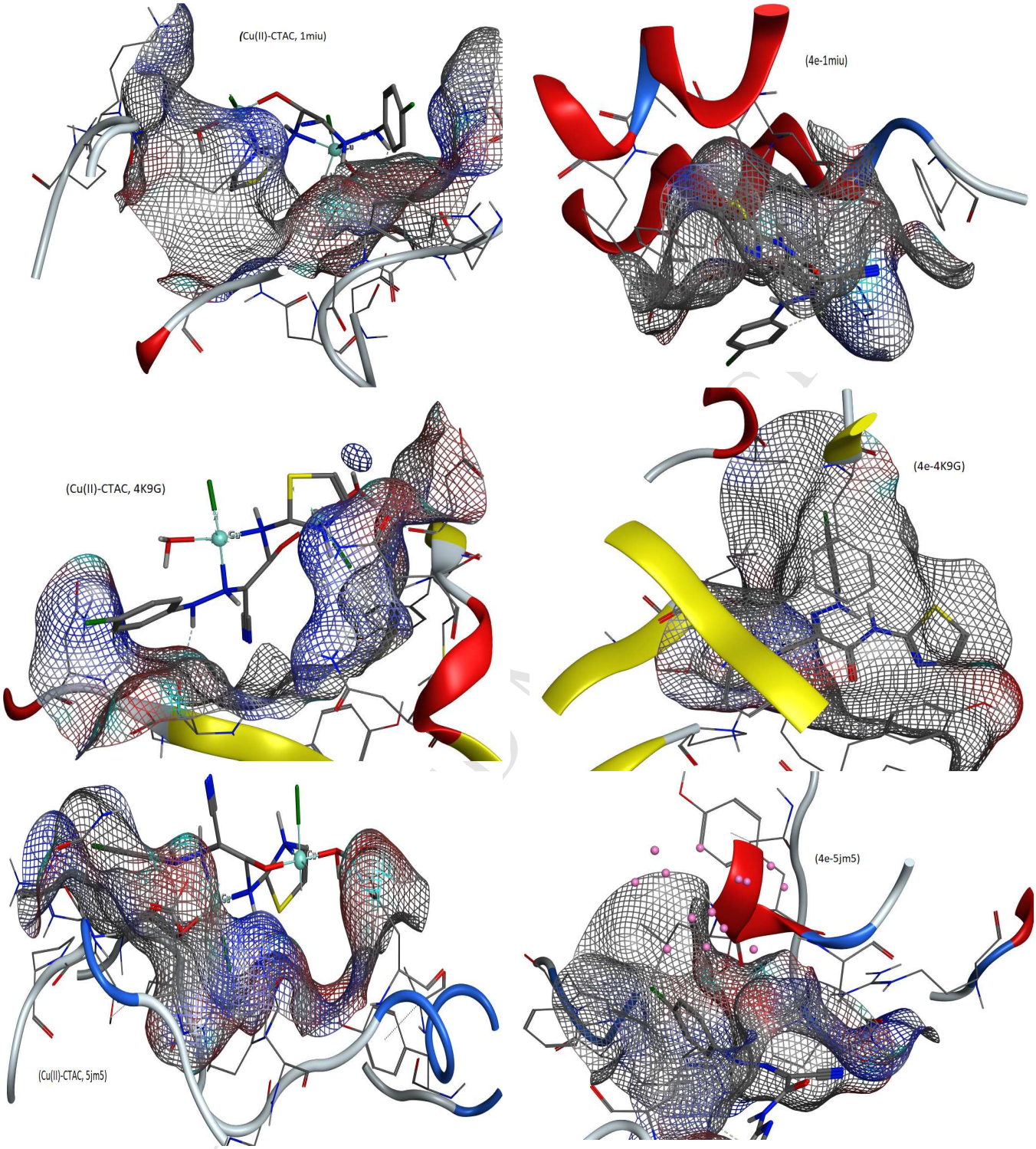

Fig.10. Surfaces and maps of selected inhibitors in binding sites against three cancer proteins

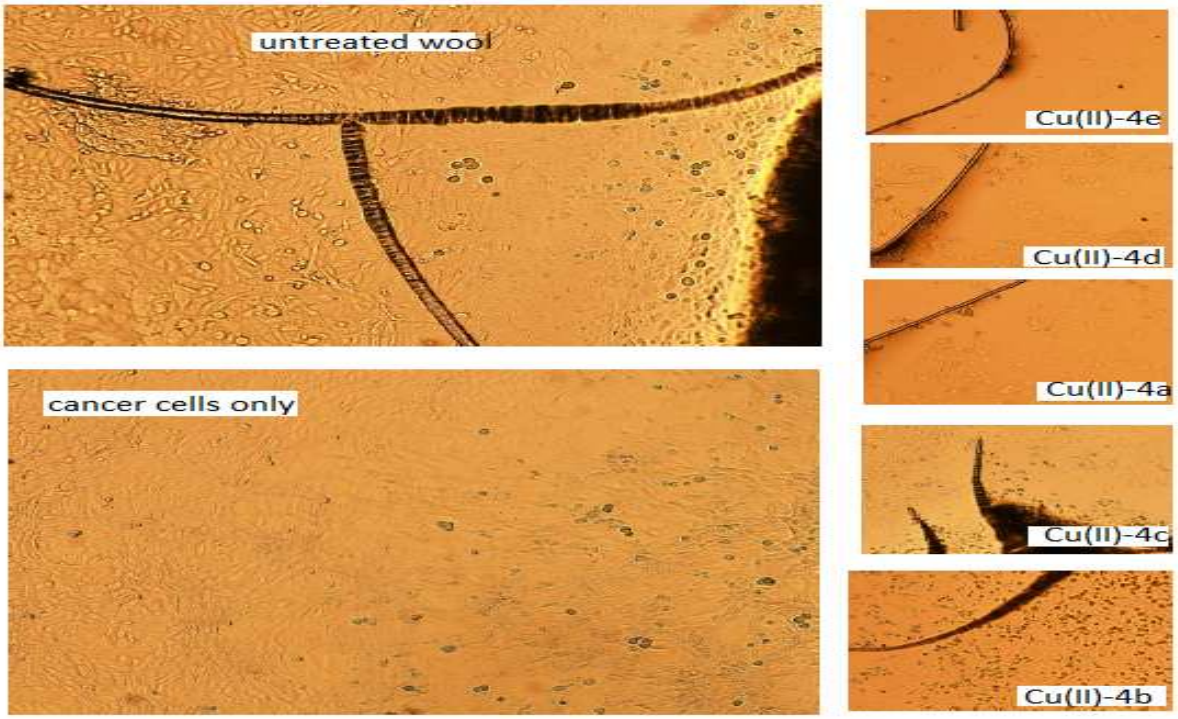

Fig. 11. Spectroscopic monitoring for dyed cotton fabric using Cu(II)-thiazole complexes against HCT-116 cell line

1- Synthesis for new Cu(II)-thaizole complexes
2- All synthesized were characterized using possible tools
3- Gaussian09 software, was used to optimize the structural forms
4- MOE module, was used for docking process as a preliminary step before antitumor application
5- The complexes were screened against three carcinoma cell lines as well as healthy cell line
6- After dyeing the cotton fabric, such fabric was tested as a special bandage for cancerous wounds